REPUBLIC OF TURKEY
ISTANBUL GELISIM UNIVERSITY
INSTITUTE OF GRADUATE STUDIES

Department of Electrical and Electronics Engineering

AN IMPROVED MAXIMUM POWER POINT TRACKING FOR A PHOTOVOLTAIC SYSTEM WITH CURRENT SENSOR-LESS FOR SOLAR WATER PUMPING SYSTEM APPLICATION

Master Thesis

Zainab Turki Idan RABEEAH

Supervisor

Asst. Prof. Dr. Yusuf Gürcan ŞAHIN

Istanbul - 2023

THESIS INTRODUCTION FORM

Name and Surname	**:**	Zainab Turki Idan RABEEAH
Language of the Thesis	**:**	English
Name of the Thesis	**:**	An Improved Maximum power point tracking for a photovoltaic system with current sensor-less for solar water pumping system application
Institute	**:**	Istanbul Gelisim University Institute of Graduate Studies
Department	**:**	Electrical and Electronics Engineering
Thesis Type	**:**	Master
Date of the Thesis	**:**	05/09/2023
Page Number	**:**	79
Thesis Supervisors	**:**	Asst. Prof. Dr. Üyesi Yusuf Gürcan ŞAHIN
Index Terms	**:**	Singel sensor MPPT,BLDC motor,Boost converter DC-AC inverter,Photovoltic(PV).

Turkish Abstract **:** Bu makale, fırçasız DC (BLDC) motor kullanan bir su pompalama sistemini (WPS) besleyen bir fotovoltaik sistem (PVS) için basit ve ucuz bir maksimum güç noktası izleme (MPPT) yöntemi önermektedir. MPPT yöntemi, motoru besleyen gerilim kaynaklı invertör (VSI) için gerekli DC bara gerilimini de sağlayan bir yükseltici dönüştürücünün yardımıyla gerçekleştirilir. . Ayrıca BLDC motorun kötü hava koşullarındaki performansını artırmak için pil enerji depolama sistemi (BESS) tabanlı lityum pil PVS ile entegre edildi. Ayrıca önerilen WPS, PVS ve BLDC motorun performansını göstermek amacıyla farklı ışınım seviyeleri altında

tasarlanmış ve test edilmiştir. Simülasyon sonuçları MATLAB yazılım programı kullanılarak elde edilmiştir. Önerilen MPPT'nin çeşitli iklimlerde PV sistem tabanlı WPS'nin işlevselliğini artıracağı gösterilmiştir. Geleneksel P&O MPPT ile yapılan bir karşılaştırma, önerilen tekniğin daha hızlı yakınsadığını ve çevresel koşullar değiştiğinde bile PV gücünde iyi bir kararlı durum salınımını koruduğunu göstermektedir. Ek olarak, önerilen yöntem PV gücünde mükemmel bir salınım sağlar**.**

Anahtar Kelimeler- tek sensör, maksimum güç noktası takibi, fotovoltaik, su pompalama, BLDC motor, boost dönüştürücü, akım sensörsüz, akü.

Distribution List **:**

1. To the Institute of Graduate Studies of Istanbul Gelisim University
2. To the National Thesis Center of YÖK (Higher Education Council)

Zainab Turki Idan

REPUBLIC OF TURKEY
ISTANBUL GELISIM UNIVERSITY
INSTITUTE OF GRADUATE STUDIES

Department of Electrical and Electronics Engineering

AN IMPROVED MAXIMUM POWER POINT TRACKING FOR A PHOTOVOLTAIC SYSTEM WITH CURRENT SENSOR-LESS FOR SOLAR WATER PUMPING SYSTEM APPLICATION

Master Thesis

Zainab Turki Idan RABEEAH

Supervisor

Asst. Prof. Dr. Yusuf Gürcan ŞAHIN

Istanbul - 2023

DECLARATION

I hereby declare that in the preparation of this thesis, scientific ethical rules have been followed, the works of other persons have been referenced in accordance with the scientific norms if used, there is no falsification in the used data, any part of the thesis has not been submitted to this university or any other university as another thesis.

Zainab Turki Idan

05/09/2023

TO ISTANBUL GELISIM UNIVERSITY
THE DIRECTORATE OF GRADUATE EDUCATION INSTITUTE

The thesis study of Zainab Turki Idan RABEEAH titled as An Improved Maximum Power Point Tracking For A Photovoltaie System With Current Sensor Less For Solar Water Pumping System Application has been accepted as MASTER in the department of Electrical-Electronic Engineering by out jury.

Director _____

Asst. Prof. Dr. Yusuf Gurcan SAHIN

(Supervisor)

Member _____

Asst. Prof. Dr. Sevcan KAHRAMAN

Member _____

Asst. Prof. Dr. Kenan BUYUKATAK

APPROVAL

I approve that the signatures above signatures belong to the aforementioned faculty members.

... / ... / 20..

Prof. Dr. Izzet GUMUS

Director of the Institute

SUMMARY

Today, several different maximum power point tracking (MPPT) techniques for extracting the greatest power from photovoltaic (PV) arrays have been created by employing both voltage and current sensors. The implementation circuit of these techniques may present high cost and large size. Therefore, in this thesis an improved MPPT technique for a PV system with a single voltage sensor is proposed. To sense the PV voltage, simply and low cost sensor such as voltage divider circuit is needed in this technique without needing for the additional current sensor. For this reason, this thesis proposes a straightforward and inexpensive MPPT method for a PV system that feeds a water pumping system (WPS) that uses a brushless DC (BLDC) motor. The MPPT method is carried out with the assistance of a boost converter, which also supplies the necessary DC bus voltage for the voltage source inverter (VSI) that supplies the motor. In addition, the battery energy storage system (BESS) based lithium battery was integrated with the PVS to enhance the performance of the BLDC motor under bad weather conditions. Moreover, the suggested WPS is designed and tested under different irradiance levels to show the performance of the PVS and the BLDC motor. The simulation results are obtained using MATLAB software program. It has been shown that the proposed MPPT would enhance the functionality of PV system-based WPS in a variety of climates. A comparison with the traditional P&O MPPT demonstrates that the suggested technique converges more rapidly and keeps a good steady state oscillation in the PV power even when environmental circumstances change. Additionally, the proposed method maintains an excellent oscillation in the PV power.

Key Words: maximum power point tracking, single voltage sensor, photovoltaic, water pumping system, BLDC motor

ÖZET

Günümüzde fotovoltaik (PV) dizilerden en yüksek gücü elde etmek için hem voltaj hem de akım sensörleri kullanılarak birkaç farklı maksimum güç noktası izleme (MPPT) tekniği oluşturulmuştur. Bu tekniklerin uygulama devresi yüksek maliyetli ve büyük boyutlu olabilir. Bu nedenle, bu tezde tek voltaj sensörlü bir PV sistemi için geliştirilmiş bir MPPT tekniği önerilmektedir. Bu teknikte PV gerilimini algılamak için ek akım sensörüne ihtiyaç duymadan, gerilim bölücü devre gibi basit ve düşük maliyetli bir sensöre ihtiyaç duyulmaktadır. Bu nedenle bu tez, fırçasız DC (BLDC) motor kullanan bir su pompalama sistemini (WPS) besleyen bir PV sistemi için basit ve ucuz bir MPPT yöntemi önermektedir. MPPT yöntemi, motoru besleyen gerilim kaynaklı invertör (VSI) için gerekli DC bara gerilimini de sağlayan bir yükseltici dönüştürücünün yardımıyla gerçekleştirilir. Ayrıca BLDC motorun kötü hava koşullarındaki performansını artırmak için pil enerji depolama sistemi (BESS) tabanlı lityum pil PVS ile entegre edildi. Ayrıca önerilen WPS, PVS ve BLDC motorun performansını göstermek amacıyla farklı ışınım seviyeleri altında tasarlanmış ve test edilmiştir. Simülasyon sonuçları MATLAB yazılım programı kullanılarak elde edilmiştir. Önerilen MPPT'nin çeşitli iklimlerde PV sistem tabanlı WPS'nin işlevselliğini artıracağı gösterilmiştir. Geleneksel P&O MPPT ile yapılan bir karşılaştırma, önerilen tekniğin daha hızlı yakınsadığını ve çevresel koşullar değiştiğinde bile PV gücünde iyi bir kararlı durum salınımını koruduğunu göstermektedir. Ek olarak, önerilen yöntem PV gücünde mükemmel bir salınım sağlar.

Anahtar Kelimeler: maksimum güç noktası takibi, tek voltaj sensörü, fotovoltaik, su pompalama sistemi, BLDC motor

TABLE OF CONTENTS

CHAPTER FOUR
RESULTS AND DISCUSSION

ABBREDIVATIONS

MPPT	**:**	Maximum power point tracking
PV	**:**	Photovoltaic
PVS	:	Photovoltaic system
HC	**:**	Hill-climbing
IC	**:**	Incremental conductance
P&O	**:**	Petrub and Observe
FL	**:**	Fuzzy logic
ANN	**:**	Artificial neural network
GWO	**:**	Grey wolf optimization
PSO	**:**	Particle swarm optimization
WPS	**:**	Water pumping system
PI	**:**	Proportional integral
SPVWM	**:**	Space vector pulse width modulation
IMD	**:**	Induction motor drive
FOCV	**:**	Fractional open-circuit voltage
DC	**:**	Direct current
AC	**:**	Alternating current
PMDC	**:**	Permanent Magnet DC motor
GSA	**:**	Gravitation search algorithm
SRM	**:**	Switch reluctance motor
PVPEMFC	**:**	Proton exchange membrane fuel cell
DTC	**:**	Direct torque control
BLDC	**:**	Brushless DC motor
GSS	**:**	Golden-section search
THD	**:**	Total harmonic distortion
CSO	**:**	Cuckoo swarm optimization
COG	**:**	Center of gravity
VSI	**:**	Voltage source inverter
CIS	**:**	Copper indium diselenide
CdTe	**:**	Cadmium crystalline

Si	**:**	Silicon
IM	**:**	Induction motor
AI	**:**	Artificial intelligent
BESS	**:**	Battery energy storage system
EMF	**:**	Electromotive force
STD	**:**	Stead state circumstance
SSA	**:**	Slap swarm optimization

LIST OF TABLES

LIST OF FIGURES

PREFACE

This article proposes a straightforward and inexpensive maximum power point tracking (MPPT) method for a photovoltaic system (PVS) that feeds a water pumping system (WPS) that uses a brushless DC (BLDC) motor. The MPPT method is carried out with the assistance of a boost converter, which also supplies the necessary DC bus voltage for the voltage source inverter (VSI) that supplies the motor. . In addition, the battery energy storage system (BESS) based lithium battery was integrated with the PVS to enhance the performance of the BLDC motor under bad weather conditions. Moreover, the suggested WPS is designed and tested under different irradiance levels to show the performance of the PVS and the BLDC motor. The simulation results are obtained using MATLAB software program. It has been shown that the proposed MPPT would enhance the functionality of PV system-based WPS in a variety of climates. A comparison with the traditional P&O MPPT demonstrates that the suggested technique converges more rapidly and keeps a good steady state oscillation in the PV power even when environmental circumstances change. Additionally, the proposed method maintains an excellent oscillation in the PV power.

INTRODUCTION

In terms of solar power, the photovoltaic (PV) system is by far the most well-known. The term "photovoltaic" refers to solar electric systems that convert solar radiation into electricity; the phrase comes from the Greek words for "light" (photo) and "voltaic" (electricity) (voltage). Using the PV effect, sunlight is transformed into electricity inside the PV cell. Considering the average PV cell generates just 1–2 W of electricity (Murshid, Shadab, and Singh11, 2019, p. 1323-1331). PV cells are combined into modules, and arrays of modules are linked together, to increase the power output of the system (Murshid, Shadab, and Singh,2019,p. 12129) . These modules are connected to the DC bus via a DC/DC converter to supply the required load. Also, the DC/AC inverter is very important for the home energy production, standalone application or grid tied application and therefore it represents the main core of the PV systems in different applications such as water pumping systems (WPS). The typical diagram of the PV system can be shown in Fig.1.

Energy production from a PV system is very sensitive to both the amount of available sunlight and the ambient temperature. That's why as the temperature around a PV system rises, the voltage drops and the current rises somewhat. In turn, this has a dampening impact on the efficiency of PV power generation. Yet, when solar irradiation rises, the current through the PV system rises as well, with a direct proportion to solar irradiation, whereas the voltage via the PV system changes only little. In addition, the DC/DC boost converter is theoretically examined to improve the performance of the PV system based maximum power point tracking (MPPT) method for PV systems. However, better MPPT algorithms are used to optimize the PV system's output power over a wide range of solar irradiation and temperature conditions. Fig.2. shows the classification of the recent MPPT methods for the PV system. This classification has been developed and categorized into three broad categories: (i) offline or indirect MPPT techniques; (ii) online or direct MPPT methods; and (iii) intelligent MPPT methods .

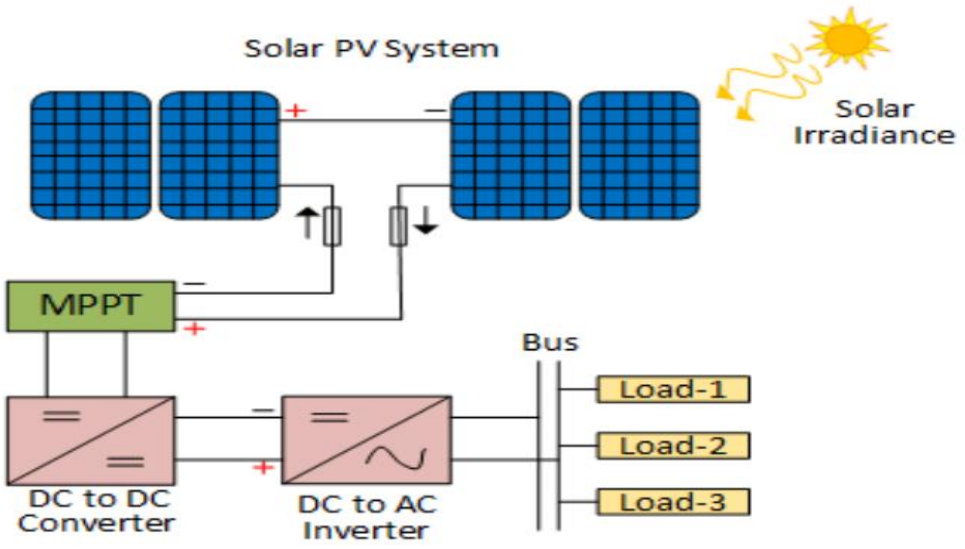

Figure 1. Typical solar PV system components (Yaqoob, Motahhir, an Agyekum,2022,p 13007)

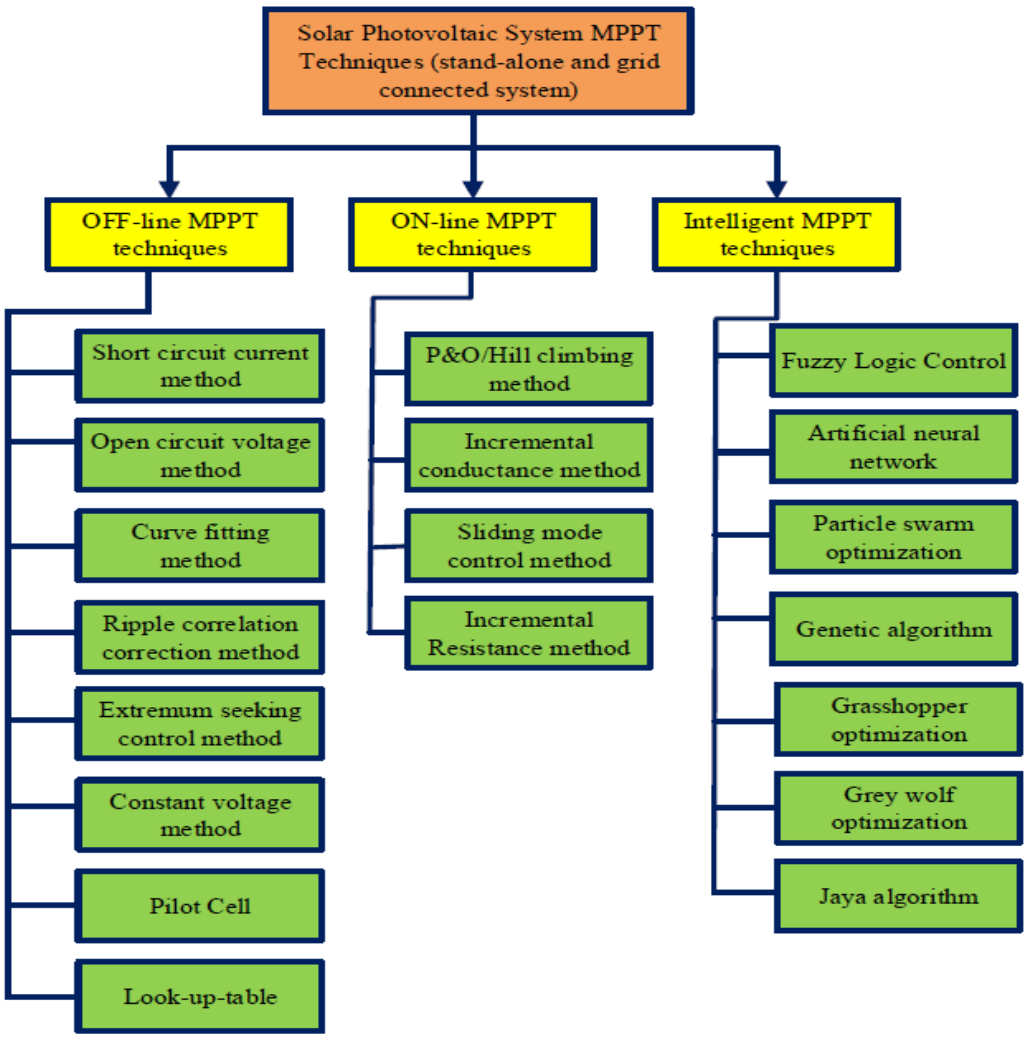

Figure 2 classification of the MPPT methods (Yaqoob, and Obed,2022,p.39-51)

The offline methods are presented by removing the PV panel from the circuit, this technique may take a reading of the open circuit voltage or short circuit current (also referred to as off-line parameters). These methods named because the PV panel is isolated from the rest of the system during the computation. These MPPT methods do not constantly monitor the voltage or current, but instead use a priori information to calculate MPP. The primary advantage of these techniques is that fewer voltage and/or current sensors are needed.

In on-line methods, the combination with the produced control signal, a small, calculated, and preset change is made to the PV system's voltage, current, or duty cycle to calculate the output power. As a result, analyzing the response of the PV panel's output power to a disturbance establishes the direction of change (increase or decrease) in the control signal. These MPPT strategies monitor MPP with no need for empiricism in beforehand. These techniques also maintain their accuracy throughout a wide range of temperatures and light levels. Methods such as hill-climbing (HC), perturb and observe (P&O), and incremental conductance (IC) are examples of MPPT strategies that fit into this category (Rasheed, Shihab, Rasheed, and Maalej 2019,p.70) .

On the other hand, successfully monitoring the global MPP in adverse weather is a major concern since typical MPPT techniques are inefficient and may become stuck between local MPP. One practical approach to determining GMPP in the presence of non-uniform solar irradiation and partial shadowing is to use intelligent algorithms. Both artificial evolutionary algorithms and genetic programming are part of the clever MPPT methods. The fuzzy logic (FL), artificial neural network (ANN), particle swarm optimization (PSO), and grey wolf optimization (GWO) etc., are all examples of MPPT methods that fall into this group. Intelligent MPPT techniques are employed in non-uniform and shaded sunlight circumstances to solve the aforementioned problem (Shongwe , Samkeloso and Moin 2015, p.938-946).

CHAPTER ONE

LITERATURE REVIEW

1.1 Literature Review

Nowadays, water pumping systems (WPS) with solar PV generation source are most used due to the solar source is free, clean, and do not have carbon emissions. Moreover, the PV systems needs minimum mechanical installation and small area working compared to other renewable energy sources such as Wind turbines. Several researchers are presented WPS with the an efficient MPPT method based PV cells to enhance the overall efficiency and transferred a maximum power to the load through power converters such as DC/ DC converter and motor drives.

Chauhan U et. al (Yaqoob, Ameer, Motahhir, Agyekum, Nayyar, and Qureshi 2021,p.1-14) proposed an improved IC based MPPT method to improve the efficiency with which a PV array uses the electricity it generates; the primary goal of this effort was to develop a robust MPPT algorithm. Thus, an IC with proportional-integral (PI) MPPT controller was presented, which is an enhanced incremental conductance MPPT controller. Traditional MPPT techniques, such as IC and P&O have a straightforward design and are straightforward to execute. Low tracking efficiency and steady-state oscillations are problems for these algorithms. These issues are resolved, and the straightforward structure is maintained, using the suggested method. GWO is used to fine-tune the controller's settings. Using a multi crystal solar panel (KC130GT by M/S Kyocera) and the suggested algorithm, we test the INC-PI MPPT's power tracking capabilities under different irradiance patterns. The proposed method outperforms the state-of-the-art in terms of settling time, undershoot, and rising time.

Jana S et. al (Kottas,., Boutalis, and Karlis 2006,p.793-803). proposed a modified (M-MPPT) based application of a boost converter in order to extract power from a PV module in the presence of varying solar irradiation and load disturbances. For example, if the amount of solar radiation were to increase, the MPPT algorithm based on the P&O technique would experience a drift. This skew occurs when the duty cycle shifts in response to a sudden increase in solar radiation. To counteract the drift effect, a P&O-based MPPT that takes into account variations in current (dI) as well as power (dP) and voltage (dV) is created. In the study, the new MPPT is developed as innovative drift

avoidance P&O M-MPPT method for boost converter ant it compared with the standard P&O algorithm. The simulation findings are then verified by comparing them to the experimental prototype. A dSPACE 1104 is used to realize the aforementioned strategies.

In (Saleh, Obed, Hassoun, & Yaqoob 2020, p.012152) the authors studied a WPS that uses a solar PV array and an induction motor drive (IMD), in that study an analytical technique for achieving MPPT was used.

Space vector pulse width modulation (SVPWM) is used for the three-phase inverter's signal generation gate. When applied to an IMD-based WPS, an analytical MPPT control (AMPPTC) method shows rapid dynamic performance with little overshoot. The AMPPTC technique further increases the system's stability throughout a broad speed range of IMD and renders it immune to the effects of parameter fluctuations by providing absolute steady-state resilience in the face of changes in solar irradiance/parameters. The Simulink environment of MATLAB is used to model and simulate this two-stage PV system, which consists of an MPPT-controlled boost converter and an SVPWM-based three-phase inverter that runs the pump.

Hmidet A et. al. in (Yaqoob, Hussein, & Saleh,2020) proposed a low-cost and high-performance solar-powered WPS that operates independently of the grid. To implement the suggested approach, a control technique is used that combines closed-loop scalar control with an enhanced fractional open-circuit voltage (FOCV) method for MPPT. As a result, the IM would need a speed sensor/encoder in addition to a current sensor. Moreover, a 1KVA rated prototype of the proposed off-grid solar WPS and its control system is used to verify its efficacy under steady-state and dynamic situations of insolation variation. Moreover, the drive's applicability to the task of water pumping is evaluated under a variety of operational settings, where it is shown to be sufficient. The suggested approach also ensures a quick reaction time, reduced oscillations at the MPP, 99% system efficiency, and a high flow rate as a result of maximum power extraction.

Attia H. (Shang,Guo, & Zhu,2020, p.1-8) proposed ANN MPPT method in order to provide optimal circumstances for MPPT, and therefore the system is managed by an ANN algorithm with function softening provided by a PI controller. The electricity for the water pump is planned to come from a PV array that is linked in parallel. The direct current (DC) pump is adopted to avoid the complexity of the alternating current (AC)

pumping system, which includes inverter, power filter, and insulated step up transformer. The proposed design considers a Permanent Magnet DC motor (PMDC) of 48 V, and 500 W as a water pump's motor. In that study, the PI controller is included to soften the MPPT controller performance, and a feed forward ANN type is used to provide the reference voltage for the MPPT operation of the PV system. In that study, the system is designed, and the MATLAB simulation was used to find results, and the analysis of the findings. The results of the investigation show that the proposed method works well in practice.

Priyadarshi N, et al (Baime, Tapuchi, Levron, & Belikov,2019, p.3) developed an improved CUK-SEPIC converter with MPPT is proposed for use in solar water pumps. Moreover, a novel MPPT strategy based on a combination of the gravitational search algorithm (GSA) and PSO was presented to enhance the PV's efficacy. The CUK-SEPIC power converter is used due to it has recently been shown to provide the same output whether the ground is positive or negative. By combining the inductor's input and output magnetic cores, the unique converter both reduces supply current ripple and maximizes PV power extraction from solar modules. In order to put the suggested technology through its paces, a switch reluctance motor (SRM) is used for WPS operations under varying solar insolation.

Khelifi B, et al (Sher, Murtaza, Noman, Addoweesh, Al-Haddad, & Chiaberge, 2015,p.1434-1434) proposed an efficient sliding mode ANN based MPPT for the PV system powered WPS. However, the SM-ANN-MPPT controller, it was discovered to improve the performance of PV power ripples and decreased the dissipated energy in the PV modules. The suggested controller is used for a stand-alone PV system coupled with a proton exchange membrane fuel cell (PVPEMFC), taking into account the effects of varying irradiance and temperature. The system's three-phase PMSM is specifically designed for use in solar-powered pumping applications. Direct torque control (DTC) using SVM is used to maintain PMSM control. A daily sunlight profile and an enforced speed profile are compared. Furthermore, both constant and changing load profiles are addressed. The control behavior is simulated, and the results are displayed, proving that the DTC-SVM PMSM drive is effective. In normal, everyday weather circumstances, the results demonstrate an increase in robustness and stability.

Alrajoubi H, and Oncu S (Jately, Azzopardi, Joshi, Sharma, & Arora, 2021,p.150-111467)presented a novel hybrid MPPT approach was introduced to enhance both speed

reaction and efficiency. This technique was developed to regulate a single-stage brushless DC (BLDC) motor used in a solar-powered WPS system. Removing the need for the DC-DC converter helps the system run more efficiently and saves money. To further improve system-wide efficiency, a two-mode hybrid MPPT algorithm is devised, which combines the golden-section search (GSS) and IC method. Convergence on the global peak is managed in the early stages using the GSS optimization approach, which also speeds up the process overall. The results demonstrate the suggested MPPT algorithm's capability of reliably and efficiently driving a 1150W BLDC motor with good tracking efficiency.

Oliver JS, et al (Nasser, Yaqoob, & Hassoun, 2021,p. 617-624) presented a variety of DC/DC converter topologies well-suited for BLDC motors for WPS. A MPPT mechanism that has been fine-tuned ensures the converters always work as expected based on the PI controller in conjunction with modern optimization techniques to achieve the highest possible conversion efficiency. Comparisons of converter output, motor characteristics, and grid output are provided by the findings obtained with SEPIC, LUO, and interleaved LUO converters. Three distinct converters' performance are analyzed, and many optimization techniques are tried and tested. After looking at the findings of three different converter topologies, the interleaved LUO converter performed the best results which it achieves a voltage gain ratio of 1:22, a conversion efficiency of 98.3%, and a total harmonic distortion (THD) of only 2.9% in the grid current. The proposed system also benefits from the ability to function independently or in a grid-connected configuration.

Ammar A, et al. proposed (Carlos, Giraldo, and Omar 2017,p.12)Alvarez. an enhanced MPPT approach based on cuckoo swarm optimization (CSO) method to improve the control performance in partially shaded environments. The purpose of this study is to optimize the power extraction of a solar pumping system that uses no batteries. Also, MPPT is achieved by use of a DC-DC converter. In addition, the BLDC motor is employed to improve the pumping system's dependability and make the most of the power produced by the PV array. Simulations were run in MATLAB and Simulink to test how well the suggested system would work.

Hasan M et al (Jyothy, Lakshmi, and Sindhu 2018,p.375-380) presented a two-stage control scheme is presented for a solar PV model that is coupled with a BLDC through a DC to DC zeta converter. It is suggested to create the pulse control for the zeta

converter in the first stage using MPPT based on fuzzy rules. This sophisticated control method is able to quickly and effectively harvest maximum power from a solar PV system, while also reducing the time required to do so. The center of gravity (COG) approach is utilized in the defuzzification process of FL controller, which is one of the three essential processes. The performance of the FL to extract maximal power for a solar system was analyzed under transient and dynamic conditions with varying levels of solar insolation. Moreover, in the second stage, a trapezoidal control strategy based electronic commutation is adopted to create the pulses of voltage source inverter (VSI), and it provides smooth control of the BLDC, making it suitable for use in WPS or irrigation systems... With the help of MATLAB simulations, the authors shown how well the suggested fuzzy rule based control method works in practice.

1.2 Thesis Objectives

The main aim of this research is to modeling and control of solar PV system for WPS based on BLDC motor using a low cost single-sensor MPPT method. The proposed MPPT method is designed without current sensor in the MPPT circuit and therefore this offers a costless and small size system. The objectives of this work include the following highlights:

i. Design a low cost MPPT controller for the WPS powered by PV array using IC MPPT technique with one sensor to increase efficiency of the PV system under different weather conditions.
ii. Analyze and simulate of the 3.6 KW WPS based BLDC motor by using electronic commutation method control
iii. Improve the performance of the BLDC motor by using battery energy storage system to control the DC link voltage and achieve constant speed control.

CHAPTER TWO

THEORETICAL BACKGROUND

2.1 Overview of PV cells

During the last several years, solar power has risen to prominence as one of the most promising renewable energy options. As compared to other energy sources, solar energy using PV cells has the highest availability. In a single day, the sun provides enough energy to meet all of Earth's energy demands for an entire year (Kumar, Rajan, and Singh 2017,p.222-232). Solar power is eco-friendly since it doesn't release any hazardous byproducts or pollutants into the atmosphere. Several different contexts may benefit from solar-to-electricity conversion.

Solar energy is mostly used in residential, vehicle, space and aviation, and naval applications. Solar PV, thermal power, and heating systems are just a few examples of the technologies that have been created to harness the sun's rays. Both technology advancements leading to lower costs and government regulations encouraging the development and use of renewable energy sources have contributed to the meteoric rise of solar PV and thermal power systems in recent years. Concentrated solar power and large-scale PV systems that feed into energy grids are two examples of modern solar technologies. Formerly, solar technologies comprised mostly of small-scale PV cells. In theory, solar energy might provide more power than the whole world uses. Despite the market's recent expansion and solar energy's technological promise, it still accounts for a small fraction of the world's total energy supply. Powering things like water pumps, lights, appliances, and machinery in homes and businesses requires more complex systems. These days, PV systems are also used to power numerous road and traffic signals .

2.2 PV cell/module/array

Smaller than a postage stamp and larger than several inches across, solar PV cells exist in a wide range of forms and sizes. They are often assembled into PV modules that may be as long as a few feet and as broad as a few feet. As a result, PV arrays of varied sizes and power outputs may be constructed from the PV modules by combining and connecting them. A PV system consists mostly of the modules in the array, but it may

also comprise cables, brackets, inverters, and other electrical parts (Kumar, Rajan, and Singh2017,p.222-232).

Each solar electric system begins with a single solar cell, also known as an a PV or photovoltaic cell. It is not uncommon for a single PV cell to only provide 1 or 2W of electricity. Connecting PV cells together into bigger pieces called modules is necessary to increase their power output. Moreover, these modules may be linked together to build arrays of greater size, each of which can then be connected to others to generate even more energy. The output voltage may be raised by connecting the cells or modules in series. For this reason, when cells or modules are connected in parallel, the output current may rise to greater levels. As a result, the PV modules are connected in series/parallel connection. The PV cell, module and array diagram can be seen in Fig.2.1 (Kumar, Rajan, and Singh 2016,p.1-6) .

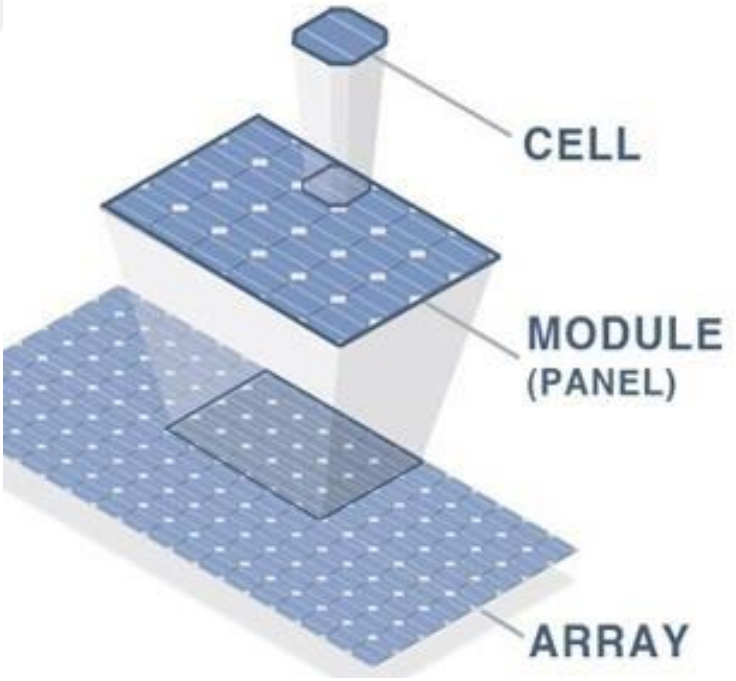

Figure 2.1 PV cell/module/array

2.3 Equivalent circuit of the PV cell

Fig. 2.2 depicts a model of a PV cell in the form of an analogous circuit. One diode is used in this variant, thus the name (Kumar, Rajan, and Singh2016 p.1-6)&(Kumar, Rajan, and Singh,2015,p.1222-1226) It depends on the hypothetically small recombination loss in the depletion zone. The one-diode model is commonly used in most PV applications. If the simulation findings are accurate, then the comparable circuit parameters will be as well. Since series and parallel resistance must be accounted when simulating a real-world PV cell in a model. Using semiconductor theory, the output current may get the fundamental equation that describes the I-V characteristic of the perfect PV cell as follows (Kumar, Rajan, and Singh 2015,p.1222-1226) :

$$I_{pv} = I_{ph} - I_d - I_{sh} \tag{2.1}$$

where V_{pv} is the output voltage of PV cell , I_{ph} is the source of photo–current, I_d is the diode current, I_{sh} is the shunt-resistor current, G is the solar irradiance, R_{sh} is the shunt resistor, and R_s is the series resistor.

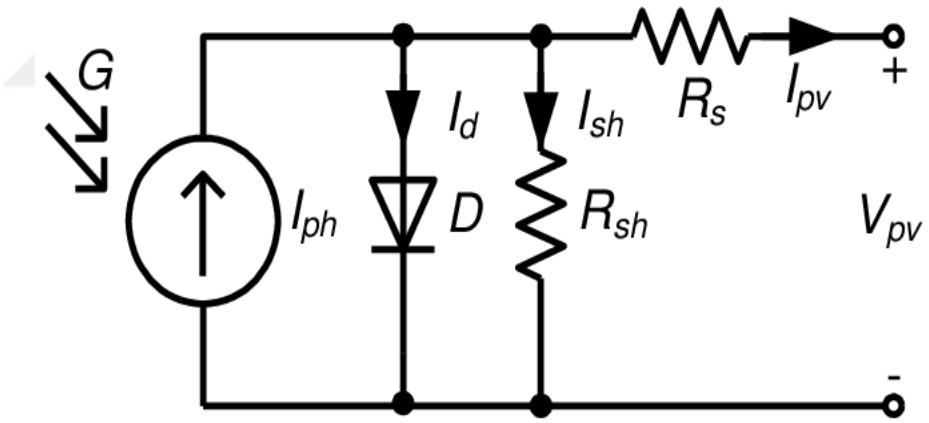

Figure 2.2 Equivalent circuit of one–diode model of PV cell.

The shunt current and diode current can replaced by their equations as below (Kumar, Rajan, and Singh 2015,p.1222-1226):

$$I_{pv} = I_{ph} - I_0 \left[exp\left(\frac{V_{pv} + R_S I_{pv}}{\gamma V_{th}} \right) - 1 \right] - \frac{V_{pv} + R_S I_{pv}}{R_{sh}} \tag{2.2}$$

Where I_0 is the saturation is current of the diode, γ is the constant of diode, V_{th} is the thermal voltage at STC conditions, and q is the electron charge. The source of

photo–current of PV module (I_{ph}) depends linearly on the solar irradiance falling on the PV module and is influenced by the ambient temperature as below(Kumar, Rajan, and Singh 2015,p.1222-1226) .

$$I_{ph} = (I_{sc} + K_i \Delta T)\frac{G}{G_n} \tag{2.3}$$

Where I_{phn} is the short-circuit current, T is the temperature, $\Delta T = T - T_n$ ($T_n = 25°C$), and G_n (1000W/m²) at STC. K_i is the coefficient for temperature at case short circuit current.

To represent the mathematical circuit of the PV array, several series panels (N_{ser}) with different parallel string (N_p) are composed to increase the output power of the PV system as seen in Fig.2.3. The PV array current can be expressed as :

$$I_{pv} = N_p I_{ph} - N_p I_0 \left[exp\left(\frac{\frac{V_{pv}}{N_{ser}} + \frac{R_s I_{pv}}{N_p}}{\gamma V_{th}} \right) - 1 \right] - \frac{V_{pv}\frac{N_p}{N_{ser}} + R_s I_{pv}}{R_{sh}} \tag{2.4}$$

The diode saturation current equation can be written as (Kumar, Rajan, and Singh 2015,p.1222-1226):

$$I_0 = \frac{(I_{sc} + K_i \Delta T)}{exp\left[\frac{(V_{oc} + K_v \Delta T)}{\gamma V_{th}}\right] - 1} \tag{2.5}$$

Where K_V represents the temperature coefficient for the case of open circuit voltage.

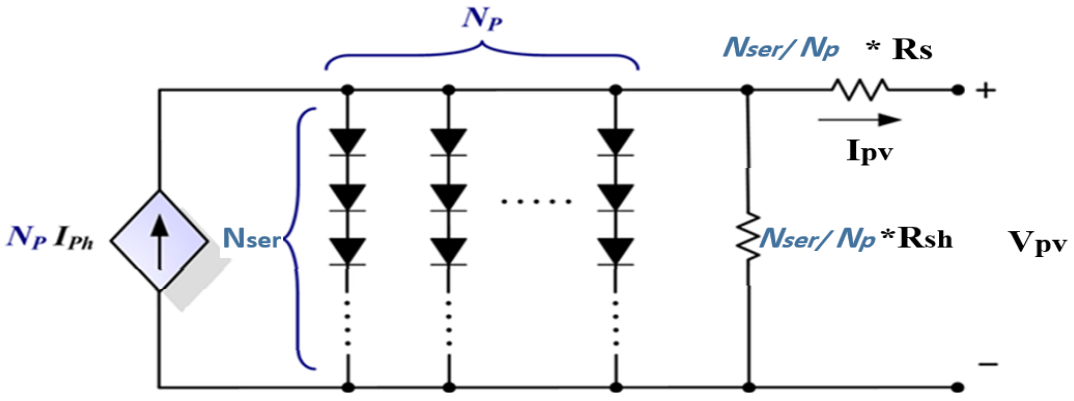

Figure 2.3 PV array model

2.4 I-V and P-V Characteristics of PV cell

In order to get a current-voltage (I-V) curve, the PV cell must be subjected to a certain amount of light, kept at a fixed temperature, subjected to a fixed amount of heat from the load, and have its output current measured at a fixed amount of voltage. Typically, there are two nodes on the I-V and P-V graphs:

• I_{sc} is the current that flows when the positive and negative terminals of the cell are connected in a short circuit or with zero load resistance.

• Open-circuit voltage (V_{oc}) is the potential difference between the positive and negative terminals when the load resistance is infinite (open circuit) and the current through the circuit is zero (Kim, Park, Lee, Ryu, and Hyun2008,p.477-487) .

The voltages and currents that may be used to run the cell are quite variable. It is possible to calculate the MPP of the cell by adjusting the load resistance anywhere from 0 (representing a short circuit) to infinity (representing an open circuit). The point on the I–V curve where the product of current and voltage is at its highest is referred to as the maximum power point (Pmp). When there is current but no voltage, also known as a short circuit, no power is created. The same is true when there is voltage but no current, known as an open circuit. Hence, the MPP lies somewhere in the middle of these two points. The "knee" of the curve is about where the maximum amount of power is produced. This point exemplifies the solar panel's capacity to convert sunlight into energy at its highest level of effectiveness as shown in Fig.2.4.

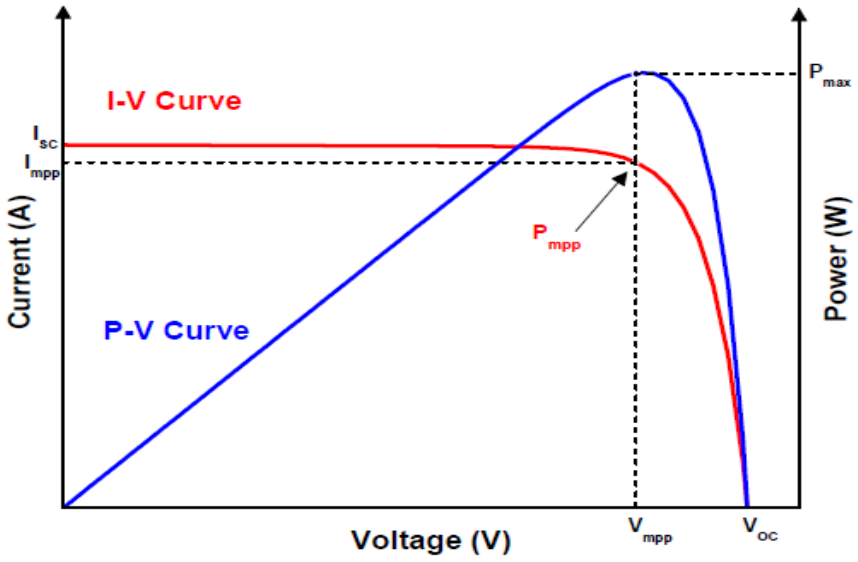

Figure 2.4 I-V and P-V typical graphs for the PV cell

2.5 PV cells materials

PV devices may be fabricated using a wide variety of semiconductor materials, which can then be deposited or organized in a number of different configurations. Silicon, polycrystalline thin films, and single-crystalline thin films are the three primary kinds of materials that are used in the production of solar cells . Silicon is the first kind, and it may be used in many different forms, including single crystalline, multicrystalline, and amorphous forms. Polycrystalline thin films are the second kind, and this section will specifically examine copper indium diselenide (CIS), cadmium telluride (CdTe), and thin-film silicon. The third and last category of material is single-crystalline thin film, with a particular emphasis on cells constructed from gallium arsenide (GaAs) (Kumar, Rajan, and Singh 2017,p.222-232).

Silicon (Si): it is a material that may have a single crystalline structure, many crystalline structures, or an amorphous structure. Silicon, which was used in the production of some of the early PV systems, is still the most prevalent material for the production of solar cells. Silicon is the second-most plentiful element in the crust of the planet, after oxygen, which is the most abundant element overall. Silicon, on the other hand, has to be refined to a purity level of 99.9999% in order for it to be usable as a semiconductor material in solar cells (Kumar, Rajan, and Singh 2017,p.222-232).

Since the whole structure of single-crystal silicon is generated from the same crystal, the molecular structure of the material, which refers to the arrangement of the atoms inside the material, is consistent throughout. Its homogeneity is perfect for maximizing the efficiency with which electrons may be transferred through the material. Silicon has to be "doped" with other elements to make it either n-type or p-type before it can be used to build an efficient PV cell. In contrast, semicrystalline silicon is made up of multiple smaller crystals or grains, which create boundaries between the individual crystals. These limits prevent electrons from flowing freely and urge them to recombine with holes, which lowers the amount of electricity that can be produced by the solar cell. The production of singlecrystalline silicon is much more costly than that of semicrystalline silicon. As a result, researchers are now looking at various techniques to lessen the impact of grain boundaries.

Polycrystalline thin films: such as CIS, CdTe, and thin-film silicon, are examples of these. The invention of thin-film technology was yet another technological breakthrough that had a significant influence on the PV industry. The name "thin-film" refers to the process used to deposit the film, not the thinness of the film itself: thin-film cells are formed in extremely thin, continuous layers of atoms, molecules, or ions. As comparison to their "thick-film" counterparts, thin-film cells provide a number of benefits. For instance, they consume very little material; the thickness of the cell's active region is often just 1–10 um, while the thickness of thick films is typically 100–300 um. In most cases, the creation of thin-film cells may take place in a large-area process, which can be an automated and continuous production process. In conclusion, they are able to be deposited on materials for flexible substrates (Kumar and Singh 2016,p.2315-2322).

In addition, thin films with a single crystalline structure, including high-efficiency components like GaAs. Gallium arsenide, sometimes known as GaAs, is a compound semiconductor that is made up of a combination of the two elements gallium and arsenic. Gallium is a more uncommon metal than gold and is produced as a by-product of the smelting of other metals, most notably aluminum and zinc. Arsenic is not an extremely uncommon element, but it is very dangerous. GaAs was first created for use in light-emitting diodes, lasers, and other electronic devices that make use of light about the same time as it was initially developed for use in solar cells.

CHAPTER THREE

DESIGN ACURRENT SENSOR – LESS MAXIMUM POWER POINT TRAKING FOR A PV SYSTEM POWERED WATER PUMPING SYSTEM

3.1 Introduction

In last few years, the water pumping systems (WPS) based on the solar photovoltaic (PV) system have been one of the common popular forms applications(Murshid, Shadab, and Singh 2019,p.1323-1331).). The PV system is the main part of the WPS systems due to it represents the main electrical source. However, the amount of solar irradiation and the temperature are the primary factors that determine the amount of electricity that can be generated by a PV system.

The important part in the PV systems in order to maximize the output power and improve the performance (Kottas, Theodoros, Boutalis, and Karlis 2006,p.793-803)). The section of the MPPT has many limitations such as cost, response speed, complexity, oscillation around the MPP, sensors. The conventional MPPT techniques such as perturb and observe (P&O)(Saleh, Obed, Hassoun, & Yaqoob2020,p.1) . incremental conductance(IC)(Yaqoob, Hussein,& Saleh,2020,p.9689), fractional open-circuit voltage, fractional short-circuit current(Baimel, Tapuchi, Levron,, & Belikov,2019,p.1426-1434), Hill Climbing (HC) (Jately, Azzopardi, Sharma & Arora, 2021,p.150-111468) fuzzy logic system, neural network, adaptive fuzzy-neural are proposed and reviewed to enhance the PV efficiency.

In this thesis, we use two techniques that have good efficiency compared to the other techniques; these techniques are INC technique and Fuzzy logic technique as observed in next sections. In this work, a single sensor MPPT method has been proposed to maximize the PV power and minimize the number of the sensors used in the conventional MPPT methods. The suggested MPPT method has one voltage sensor and the using current sensor is avoided against the traditional MPPT methods which are used two sensors (voltage and current sensors).

This chapter include the mathematical analysis of the PV cell/module, conventional MPPT techniques, WPS based brushless BLDC motor, and the suggested MPPT method.

3.2 Water pumping system

The Solar WPS system, is an excellent replacement for water pumping systems that are powered by electricity or fuel. Since its inception half a century ago, this study area has been regarded as very fruitful (Kumar, Rajan, and Singh 2016,p.2315-2322). The solar PV base WPS is a coupling of a PV array and a pump. The PV array is used to create energy, which is then used to power the pump. PV cells are the fundamental part of the system since they immediately convert the solar energy that is collected from the sun into electrical energy. This energy is then used to power the pump's motor by way of a controller, which ensures that the pump continues to function normally.

There is also the possibility of using storage components in this system, such as a battery for the storage of electric charge and a reservoir for the storage of water. The needed head of the pump and the amount of discharge it must provide varies from one application to the next. In consideration of the necessary head and discharge, an appropriate pump and PV panel will be used. Figure 1 depicts the general organizational framework of the WPS. The PV system, the power control system, and the dynamic system, which includes the motor and the pump, are its three primary components (Kumar, Rajan, and Bhim Singh. 2016,p.1-6).

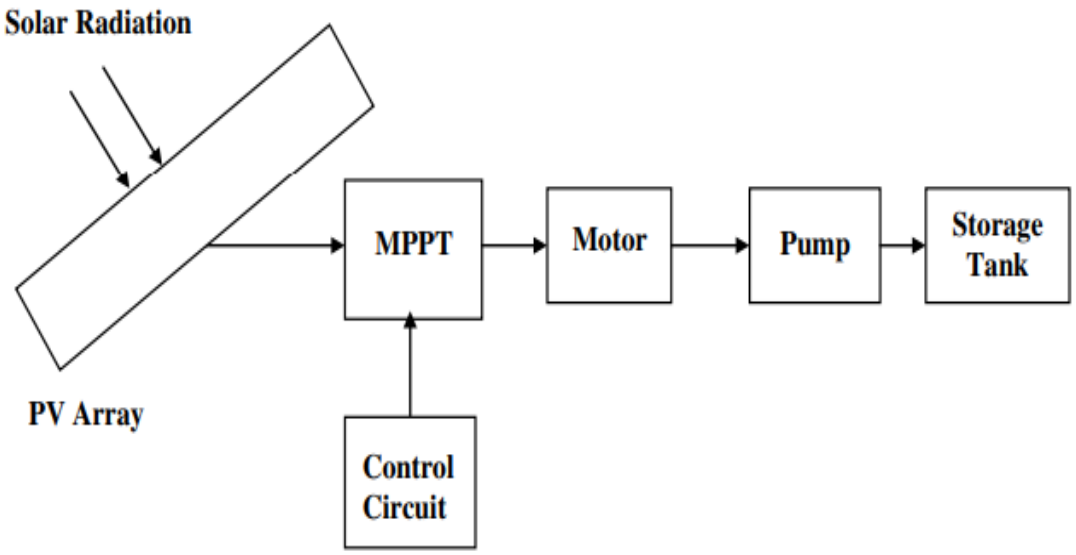

Figure 3.1 circuit components of the WPS powered by PV array

3.2.1 Brushless DC (BLDC) Motor for WPS

The brushless DC (BLDC) motor features almost minimal maintenance requirements, great dependability, high efficiency, a high torque/inertia ratio, enhanced cooling, reduced radio frequency interference, and low noise (Kumar, Rajan, and Singh 2016,p.2315-2322) . As a result of the fact that this motor has largely replaced the induction motor (IM) in a wide range of applications, including WPS (Kumar, Rajan, and Singh 2016,p.222-232) . In this work, the BLDC motor has been used to driven the water pump.

A BLDC motor's synchronizing magnetic field is generated when the stator winding interacts with the rotor's magnetic field. Because the stator windings are activated and deactivated in relation to the rotor's location, the magnetic fields produced by the rotor and the stator will be in phase with one another. To create a magnetic field in the air gap that rotates at a constant angle with regard to the field generated by the rotor, power transistors are used to electrically switch the windings(Kumar, Rajan, and Singh 2015,p.1222-1226)) . Since the BLDC motor requires for AC power source, therefore the voltage source inverter (VSI) was used to feed the motor as shown in Fig.3.2.

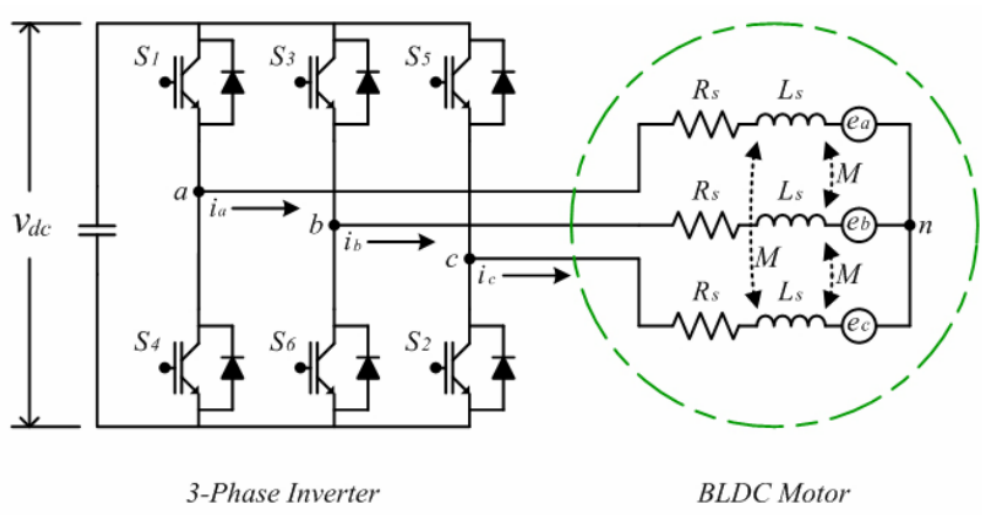

Figure 3.2 BLDC motor equivalent model

The 3-ph voltage equation may be written as (3.1) if the stator resistances of all the windings are identical and the self and mutual inductances are likewise constant. No damper windings are modelled, and neither magnets nor high-resistance stainless steel

retaining sleeves are considered in this calculation(Kim, Tae-Sung, Park, Lee, Ji-Su Ryu, and Hyun 2016,p.2315-2322) .

$$\begin{bmatrix} v_a \\ v_b \\ v_c \end{bmatrix} = \begin{bmatrix} R_s & 0 & 0 \\ 0 & R_s & 0 \\ 0 & 0 & R_s \end{bmatrix} \begin{bmatrix} i_a \\ i_b \\ i_c \end{bmatrix} + \begin{bmatrix} L_s - M & 0 & 0 \\ 0 & L_s - M & 0 \\ 0 & 0 & L_s - M \end{bmatrix} \frac{d}{dt} \begin{bmatrix} i_a \\ i_b \\ i_c \end{bmatrix} + \begin{bmatrix} e_a \\ e_b \\ e_c \end{bmatrix} \quad (3.1)$$

where v_a, v_b, and v_c represent the phase voltages, i_a, i_b, and i_c represent the phase currents, R_s and L_s are the resistance and inductance of the stator, respectively, M is the mutual inductance and , e_a, e_b, and e_c represent the phase back EMFs.

The model equation of the motor's torque is given by :

$$T_e = \frac{1}{\omega_m}(i_a.e_a + i_b.e_b + i_c.e_c) \quad (3.2)$$

Where ω_m represents the mechanical angular velocity Also, the electromagnetic torque in (N.m) of the BLDC motor can be expressed as follows:

$$T_e = T_L + J\frac{dN_r}{dt} + B_m N_r \quad (3.3)$$

Where T_L is the load torque in (N.m), N_r is the speed of the motor in (rad/sec), J is the moment of inertia in Kg.m²/rad and B_m represent the friction constant in N.m/(rad/sec). Moreover, the BLDC motor in this thesis was controlled using a VSI regulated by the electronic commutation method as seen in Fig.3.3.

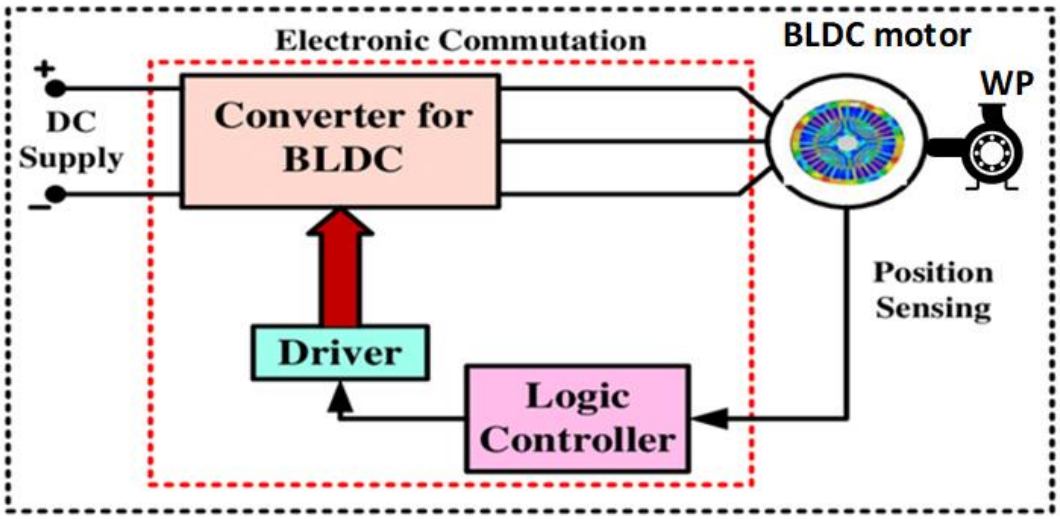

Figure 3.3 Electronic commutation method for BLDC motor control

Using a decoder logic, a BLDC motor's electronic commutation alternates the direction of the currents in its windings according to a set pattern. For each distinct range of rotor position, there is a corresponding combination of Hall-effect signals that is generated 23). The gap between these signals is 60 degrees. Table 3.1 is a tabular representation of the process whereby the assessment of rotor position leads to the development of six switching states. It is noticeable that only two switches are conducting at the same time, which leads to the 120 degree conduction mode of operation of the VSI and, as a consequence, decreased conduction losses. In addition to this, the electronic commutation allows for switching at the fundamental frequency of the VSI. As a result, the losses that are normally associated with high frequency PWM switching are minimized.

Table 3.1. States of the switching for electronic commutation of the BLDC motor

Rotor position $\boldsymbol{\theta}(°)$	**Hall signals**			**Switching states**					
	$\boldsymbol{H_3}$	$\boldsymbol{H_2}$	$\boldsymbol{H_1}$	$\boldsymbol{S_1}$	$\boldsymbol{S_2}$	$\boldsymbol{S_3}$	$\boldsymbol{S_4}$	$\boldsymbol{S_5}$	$\boldsymbol{S_6}$
$N.A$	0	0	0	0	0	0	0	0	0
$0-60$	1	0	1	1	0	0	1	0	0
$60-120$	0	0	1	1	0	0	0	0	1
$120-180$	0	1	1	0	0	1	0	0	1
$180-240$	0	1	0	0	1	1	0	0	0
$240-300$	1	1	0	0	1	0	0	1	0
$300-360$	1	0	0	0	0	0	1	1	0
$N.A$	1	1	1	0	0	0	0	0	0

3.2.2 Design of Water Pump

Both centrifugal and positive displacement pumps may be used in solar pumping systems, with the former being the more common kind. The centrifugal pump is the most popular because it can pump a lot of water with little effort, is cheap, simple, and needs little maintenance (24) . The below equations may be used to forecast the effectiveness of a centrifugal pump based on the values of the total head (H), the flow rate (Q), and the hydraulic power (P) .

$$Q = \left(\frac{N_r}{N_{r,ref}}\right).Q_{ref} \tag{3.4}$$

$$H = \left(\frac{N_r}{N_{r,ref}}\right)^2.H_{ref} \tag{3.5}$$

$$P = \left(\frac{N_r}{N_{r,ref}}\right)^3.P_{ref} \tag{3.6}$$

The flow rate is a direct function of the rotational velocity of the wheel, the monomeric height is a function of the speed squared, and the hydraulic power is a function of the speed cubed, according to these rules.

As the speed of the motor squares, so does the load torque applied by the centrifugal pump.

$$T_L = K{N_r}^2 \tag{3.7}$$

where K is the constant of the water pump.

3.3 Photovoltaic system

3.3.1 Parameters of the used PV module

The electrical characteristics of PV cells which depicts the I-V property of a PV cell depend on the three regions on the PV cell characteristic which are short-circuit current region, open-circuit voltage region, and the maximum power point (MPP) region. Moreover, the maximum energy that can be harvested from the PV cell is located in MPP. The predication of this point is based on the load line characteristics and the MPPT controller behavior. The parameters of the cell are the short circuit current (I_{sc}), the open-circuit voltage (V_{OC}), the maximum current value (I_{mpp}), the maximum voltage (V_{mpp}), and the maximum power (P_{mpp}).

The technical parameters of the PV module used in this work are listed in Table3.2. The configuration of the proposed system which is consists 3X6 modules in series/parallel are structured in this work based on design in section 3.5.2.

Table 3.2 Specification of the Trina-solar TSM-200DA01A PV module at STC conditions

Parameter	**Value**
P_{MP}	200 W
V_{MP}	38.2 V
I_{MP}	5.26 A
V_{oc}	46.2 V
I_{SC}	5.62 A
N_{cell}	72
N_P	3
N_{Ser}	6

3.3.2 Maximum power point tracking

Nonlinear I-V and P-V characteristics, which fluctuate with changes in solar irradiance and temperature, indicate the PV module energy may be varied with these factors (Li, X., Li, Y., Seem, J. E., & Lei, P 2011,p.803-810)&(Nayak, Mohapatra, & Mohanty,2013,p.1-6) . For this reason, a MPPT control unit should be used with the PV system via a DC/DC converter such as boost , buck or buck-boost converters to improve the efficiency and maximize the energy under various weather conditions as seen in Fig.3.7.

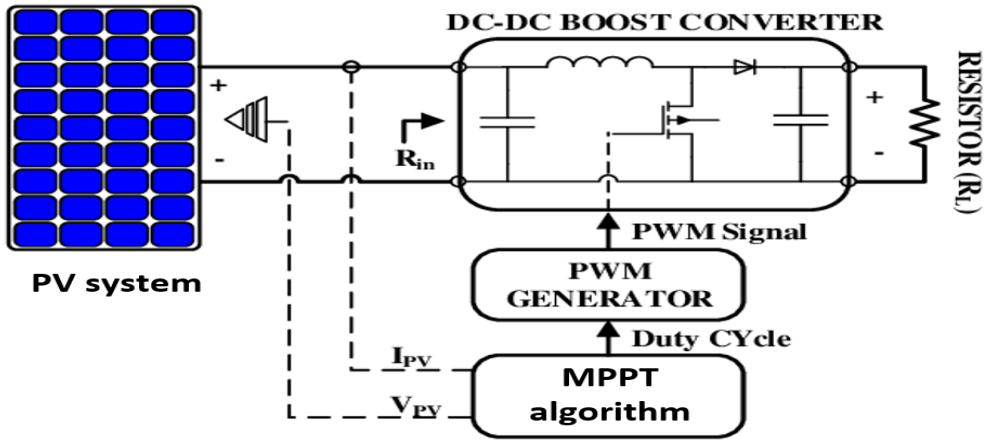

Figure 3.7 Block diagram of the PV system controlled by a MPPT control

In Fig.3.8, researchers have seen the usual I-V and P-V features of a Solar panel according to the load line specification. When a solar photovoltaic module is loaded with a variable resistance, the point where the load line and I-V curve meet is the device's optimal operating point. The AB segment of the I-V graph in this figure represents the operational point of the PV module, as shown by the slope of the properties. The operating point shifts to the right if the load resistance (R1) is small. The MPP occurs when the load resistance is equal to two times the source resistance, or (R2). Subsequently, anytime the load resistance is as big as, the operating point will shift towards the voltage zone (DE) on the curve (R3).

Furthermore, an essential rule for obtaining the greatest power point from a PV system is the load's resistance. Adjusting the load's resistance is necessary.

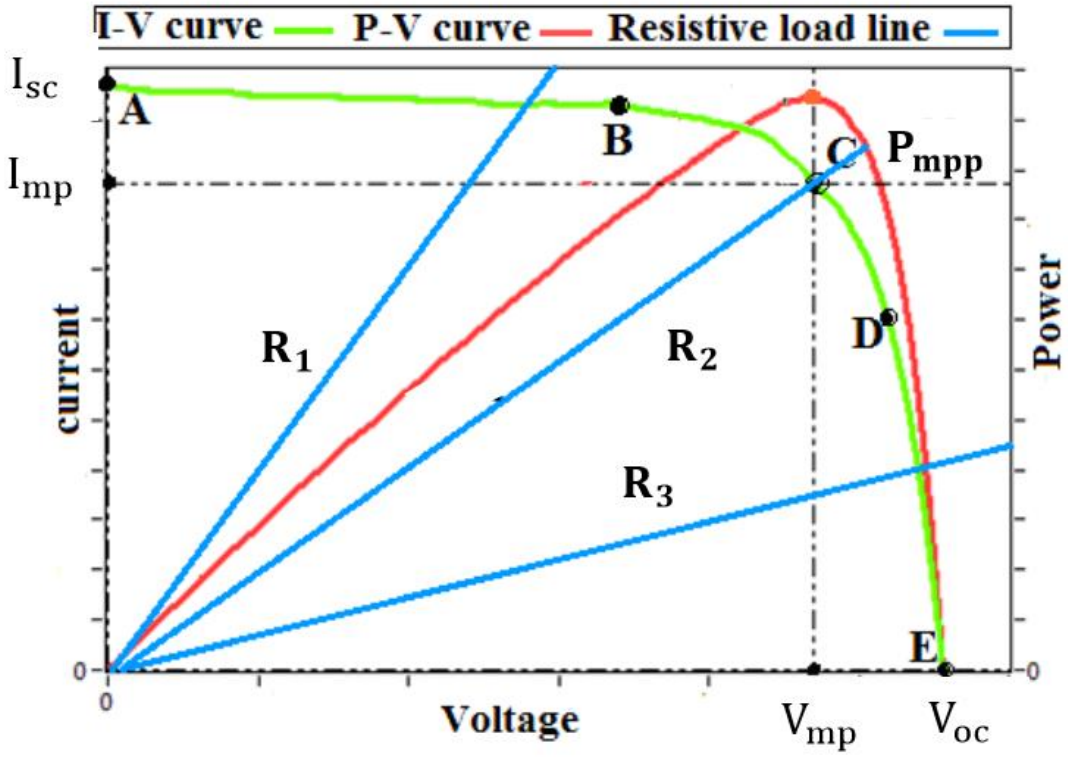

Figure 3.8 typical P-V curve of the PV system based load line characteristics

There are a lot of different MPPT approaches that can be found in the literature, and they can all be put into one of three categories: direct simple methods, artificial intelligent (AI) and MPPT based optimization methods. (Natarajan, Ramaprabha, and Ranganath 2012)(Yap, Sarimuthu, & Lim 2020,p. 1043-1059)&(Dadkhah & Niroomand,2021,p.225-236) The choice of an acceptable MPPT technique may be based on a number of factors, including the following factors:

i. The number of sensors
ii. Cost of implementation
iii. The difficulty of the implementation
iv. The capacity to recognize several local maxima that result from partial shading situations
v. Reaction time or the pace at which we converge.

However, the most used MPPT in the few last years can be given as follows:

A. Perturb and observe method

In this investigation, the P&O method is used by adjusting the boost converter's duty cycle. Figure 3.9 depicts the main algorithm used in this method . This method estimates PV power by sensing the voltage and current of the PV module. The current perturbation for P&O MPPT may be calculated once the PV power has been measured. Consider the signs of P and V to get the direction of the disturbance. If there is a rise in output, the same current perturbation is applied in the other direction to generate the subsequent PV output. In the event that the power level drops, the following PV power is calculated by applying an opposing perturbation.

The P&O approach involves the introduction of a step size ($\Delta D = 0.001$) into the system. The solar module's output power shifts as a result of this disturbance. If the power grows as a result of the disturbance, the disturbance is maintained ($D + \Delta D$) in the same direction. As the power drops down after the peak is achieved, the perturbation flips directions ($D - \Delta D$) (Liu, Kang, Zhang,& Duan 2008,p.804-807) .

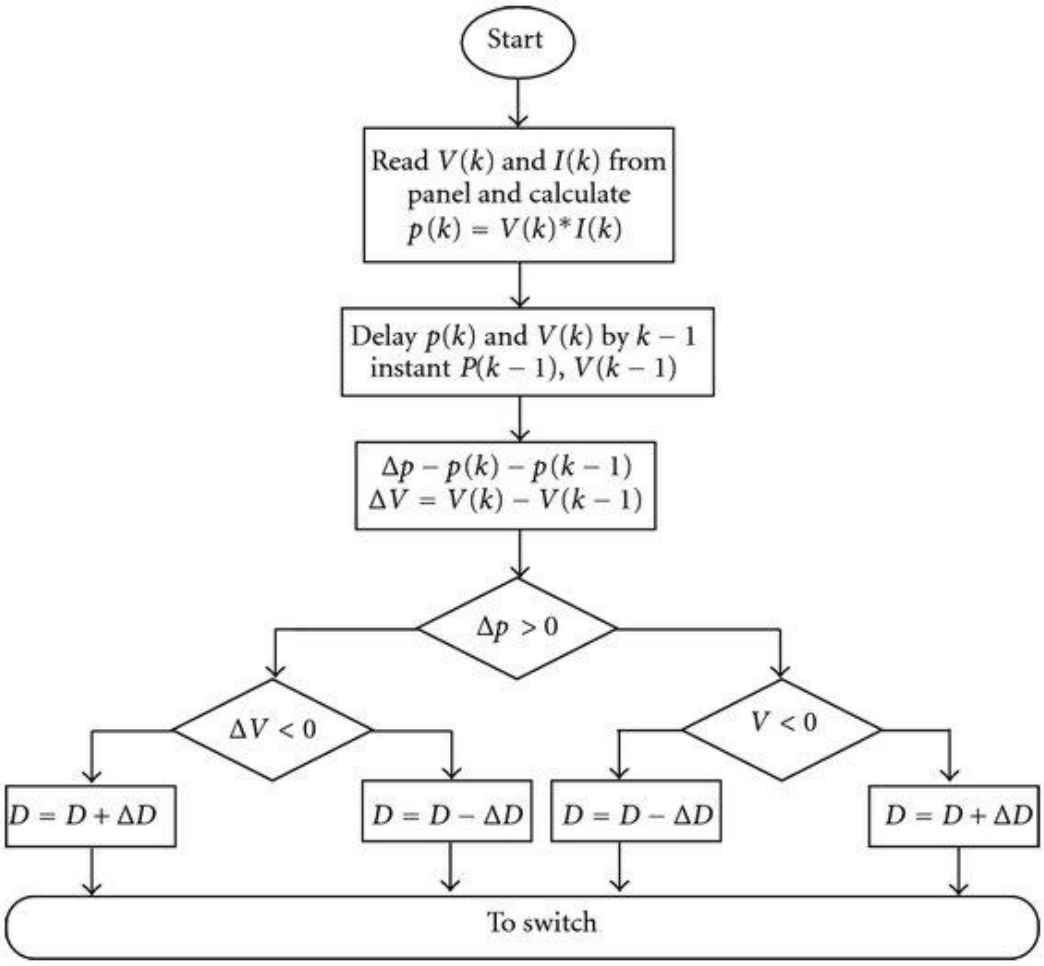

Figure 3.9 the typical flowchart of P&O (Natarajan, Ramaprabha, and Ranganath 2012)

Based on the P-V curve of the P&O MPPT as seen in Fig.3.10. The P&O starts with determining the PV output power by determining a brief disruption in the duty cycle or voltage of the DC-DC converter in a particular direction. In order to find the operating point on the P-V curve, the following conditions are necessary to obtain the MPP of the array as below:

$dP > 0$ and $dV > 0$, left of MPP

$dP > 0$ and $dV < 0$, right of MPP

$dP < 0$ and $dV > 0$, right of MPP (3.12)

$dP < 0$ and $dV < 0$, left of MPP

$dP = 0$ and $dV = 0$, at MPP

There are two significant problems with the P&O MPPT approach. The first is that, at low irradiance levels, the P&O MPPT approach does not converge on the MPP, but instead settles at a location close to the MPP since the difference between the power changes on each side of the MPP is almost nil. Second, there may be difficulty in choosing the right magnitude of perturbation, as this affects both the dynamic and steady-state responses, and it is important to strike a balance between both ((Jain, Gupta,& Bohre, 2018,p.1-6)).

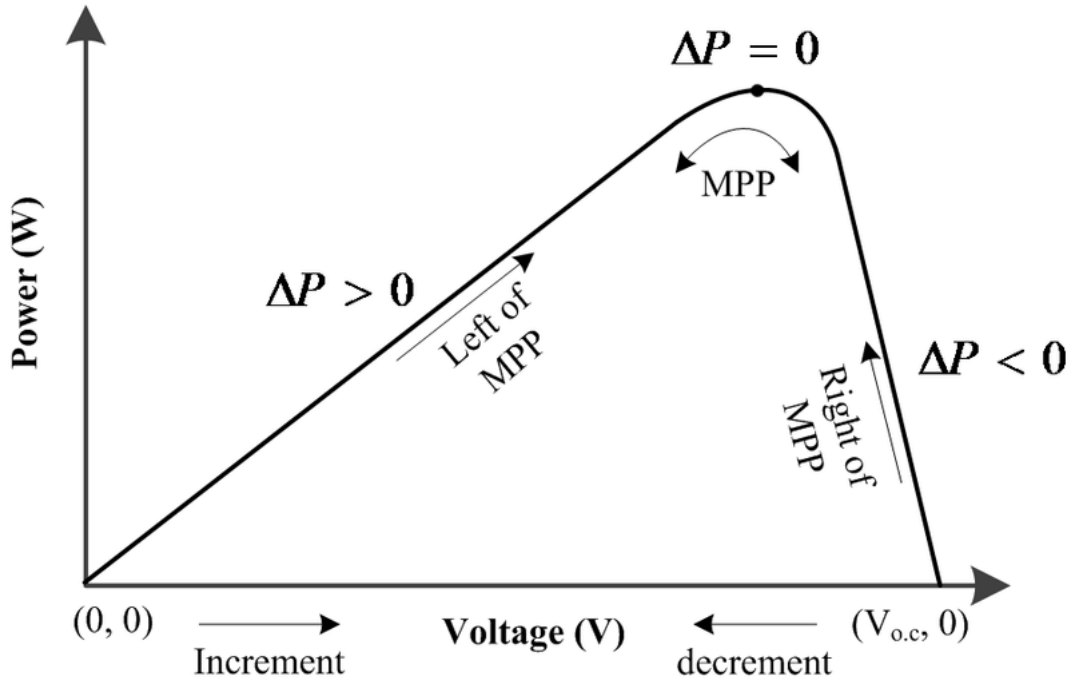

Figure 3.10. P-V curve under conventional P&O method

B. Incremental conductance Method

The fundamental objective of the INC technique is to determine the relationship between the voltage and current output of the PV panel under different environmental conditions . The ratio of the current change to the voltage change, or dI/dV, may be used to represent this condition (5) . The MPP also be calculated from the PV panel's operating point by locating the zero-derivative point, as seen in Fig. 3.11 (Liu, Kang, Zhang, & Duan 2008,p.804-807). Given that the slope of the PV curve is,

$$\frac{dI}{dV} = -\frac{I}{V}, \text{ at MPP}$$

$$\frac{dI}{dV} > -\frac{I}{V}, \text{ at left of MPP} \qquad (3.13)$$

$$\frac{dI}{dV} < -\frac{I}{V}, \text{ at right of MPP}$$

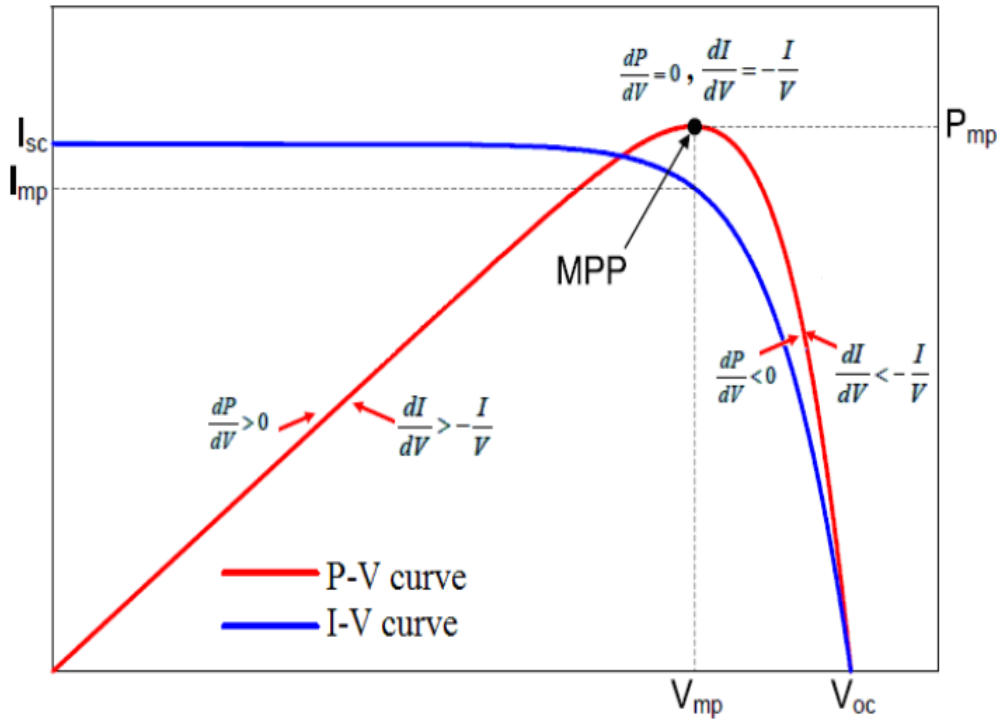

Figure 3.11. I-V and P-V characteristic for INC algorithm.

Since the improved INC MPPT method eventually converges on MPP, although with some oscillations, it effectively addresses the first issue with P&O MPPT. Nevertheless, picking an appropriate amount of increment remains a disadvantage since the incremental value of duty cycle is constant(Jain, Gupta,& Bohre, 2018,p.1-6) Fig.3.12 shows the flowchart of the conventional INC method.

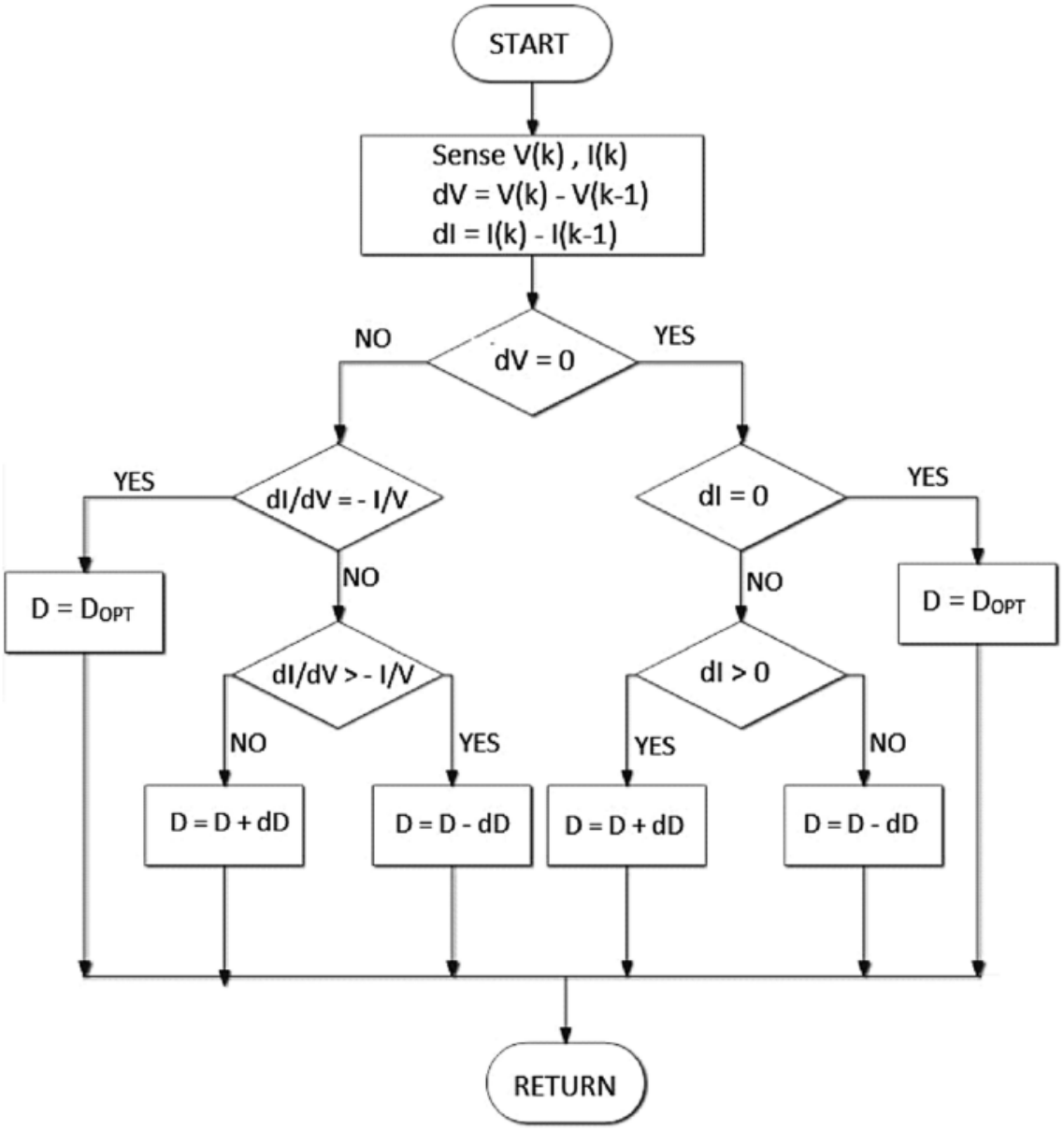

Figure 3.12 flowchart of the conventional INC method [35]

C. Fuzzy logic method

The most used AI methods is the fuzzy logic (FL) MPPT method due to it has several advantages compared with other AI techniques . Fig.3.13 shows the MPPT flowchart based FL method. Moreover, the two inputs which are the error E(k) and the change in the error ΔE is used to implement the FL algorithm. In addition, FL has single output variable, which is the change in the duty cycle ΔD for the boost converter . So, the error can be written as(Algarín, Carlos, Giraldo, and Alvarez 2017,p12) :

$$E(k) = \frac{P(k) - P(k-1)}{V(k) - V(k-1)} = \frac{\Delta P}{\Delta V} \quad (3.14)$$

Where $P(k)$ and $V(k)$ are the power and voltage of the PV panel, respectively. Also, the error can be expressed as,

$$CE(k) = E(k) - E(k-1) = \Delta E \quad (3.15)$$

The change in duty ratio has either positive or negative values, according to the position of the operational point. This result is then transferred to the dc-dc converter, which is responsible for driving the load. An accumulator was constructed by making use of the value of ΔD that was provided by Eq.(3.16) in order to acquire the value of the duty cycle.

$$D(k) = D(k-1) + \Delta D(k) \quad (3.16)$$

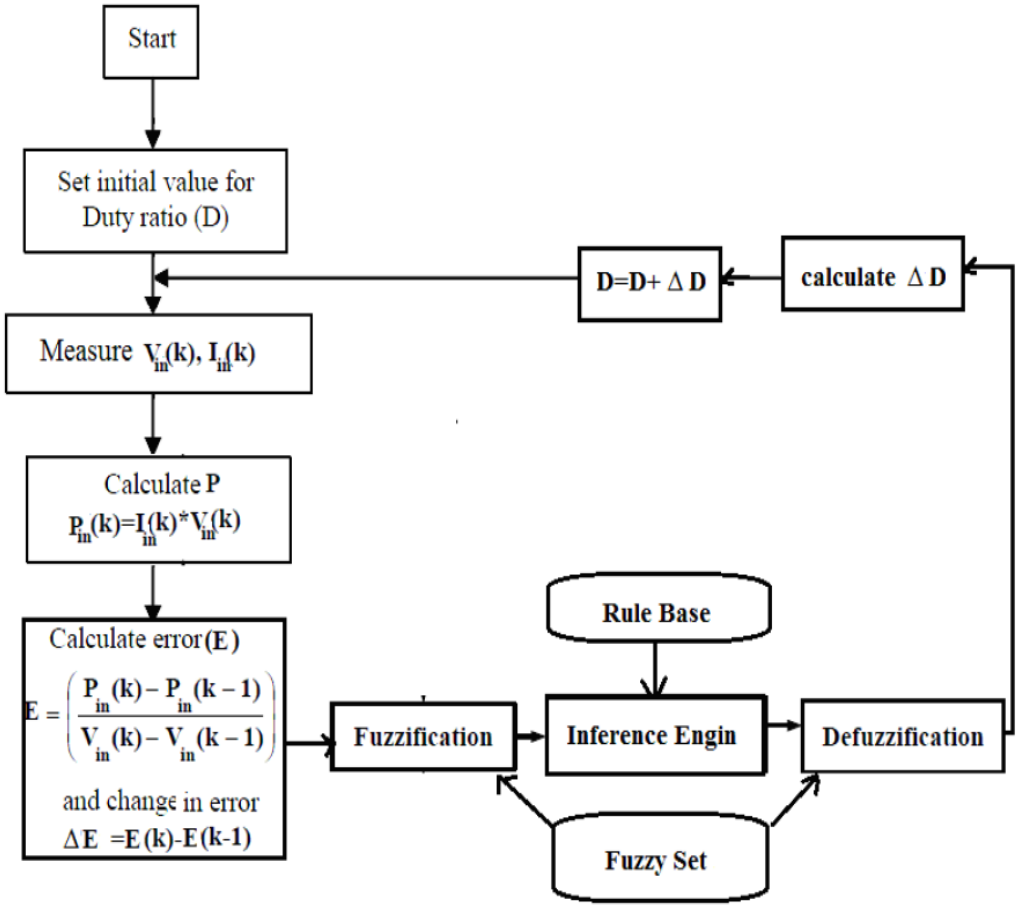

Figure 3.13 FL algorithm for the MPPT controller

3.4 Proposed WPS system based single-sensor MPPT

The proposed system configuration based on single sensor MPPT and the conventional MPPT can be seen in Fig.3.14. In the conventional WPS, the two sensors (voltage sensor and current sensor) are used to implement the MPPT algorithm. The main issue in the conventional MPPT is the high cost and the large size for the control circuit. For this reasons, the goal of this study is to minimize the cost of the control by removing the high cost current sensor from the MPPT circuit. This reduction in the cost can improve the reliability of the WPS and minimize the size system.

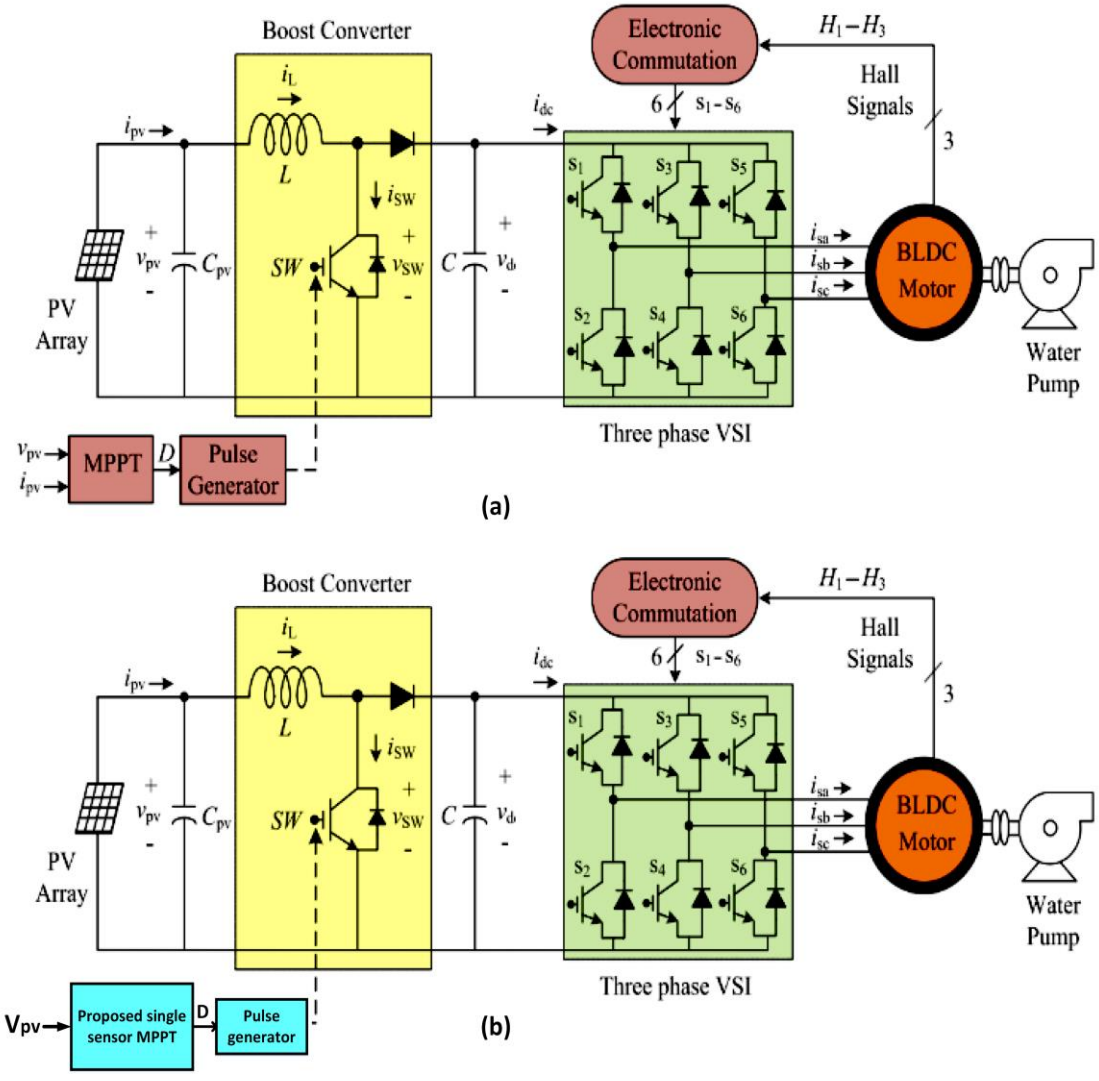

Figure 3.14. (a) WPS based PV system using conventional MPPT control (b) WPS based PV system using proposed single-sensor MPPT control.

3.4.1 Algorithm of the suggested single-sensor Method

The conventional P&O method tracks the MPP by sensing both the voltage and current and observe the PV power at fixed step size for the duty ratio and then adjust the duty by a PWM generator. The step size has to be rather tiny in order to maintain a close proximity to the MPP and to reduce the oscillations. This may have an effect on the reaction speed, which in turn results in a loss of energy. As result, it demonstrates tracking failure in the face of fast changes in environmental conditions.

The proposed single-sensor MPPT algorithm introduced in this study have operational features that are comparable to those of the INC algorithm; hence, they offer the same benefits over the standard P&O approach as the INC method. When compared to both the IC and the traditional P&O approaches, the single-sensor MPPT algorithm avoid the usage of the more expensive and complicated current sensor by using just the voltage sensor. This eliminates the need for the current sensor. This leads to a reduction in both cost and the complexity of the circuit. Therefore, the single-sensor MPPT algorithm is easier to understand and provide a better balance between their ease of use and their level of performance when compared with both the IC and the traditional P&O approaches. The suggested MPPT is designed based on the derivate the relationship between the PV voltage and the duty cycle of the boost converter. The output voltage of the boost converter was given in Eq. (3.17)(Urayai and Amaratunga 2010,p.82-88) .

$$V_o = \frac{V}{1-\delta} \tag{3.17}$$

At ideal converter (lossless case) the input power is the same output power as follows:

$$P_o = P_{in} \tag{3.18}$$

The maximum power that transfers from the PV module to the output (P_o) is achieved when Eq.(3.19) is satisfied ;

$$\frac{dP_o}{dt} = \frac{dV_o}{dt} = 0 \tag{3.19}$$

Hence,

$$\frac{dV_o}{dt} = \frac{d((V/(1-D)))}{dt} = 0 \tag{3.20}$$

Therefore, from Eq.(3.20),

$$\frac{(1-D)(dV/dt) - V(d(1-D)/(dt))}{(1-D)^2} = 0 \qquad (3.21)$$

By simplifying Eq.(12), result(Dadkhah, J., & Niroomand, M.2021,p.225-236);

$$\frac{dV}{dD} = -\frac{V}{1-D} \qquad (3.22)$$

Consequently, the criteria stated in Eq.(3.22) is satisfied at the moment at which a boost converter supplies the load with the P_{MPP}.

The flowchart of the suggested MPPT method can be seen in Fig.3.15. Moreover, the mechanism of the suggested method has layouts and features similar to that of the IC MPPT algorithm. The recommended algorithm sense only the PV module voltage whereas the conventional P&O and IC technique algorithms senses both voltage and current of the PV module.

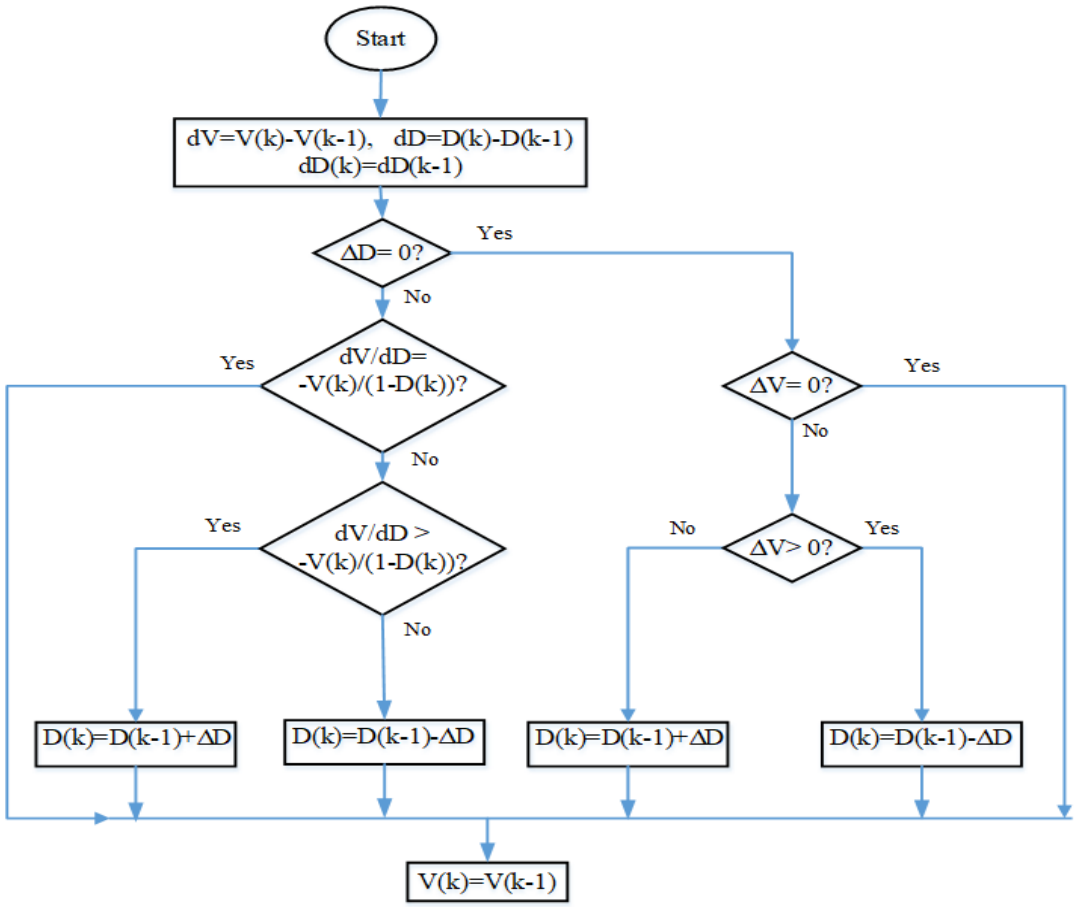

Figure 3.15 the flowchart of the proposed single sensor MPPT method

3.4.2 Design of DC/DC boost converter

The boost converter circuit is used in combination with a PV system to increase the output voltage and carry out the MPPT algorithm. Figure 3.16 shows the electrical circuit of the step-up boost converter which include input inductor, input capacitor, output capacitor, diode and controlled switch.

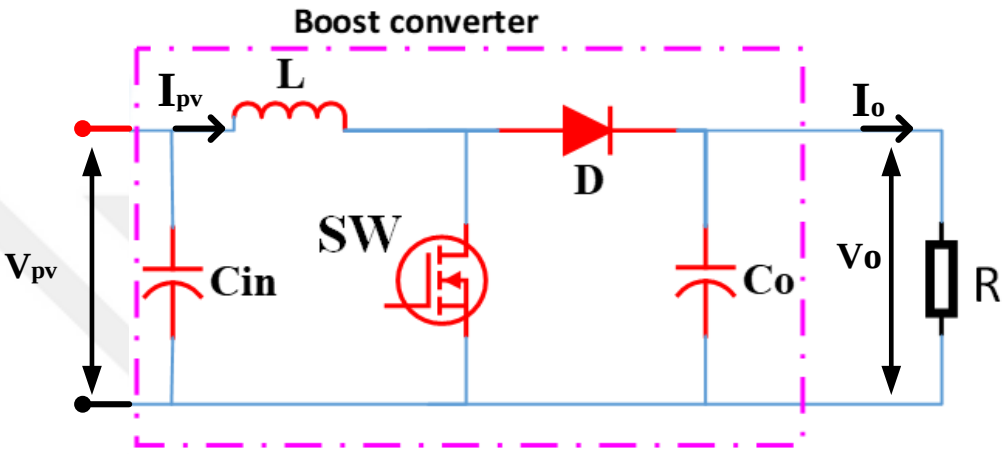

Figure 3.16 Circuit diagram of the boost converter

The voltage and current that are provided by the PV system are used to adjust the duty ratio of the boost converter. Therefore, the following design for the WPS was carried out using Eqs. (3.23-3). in order to estimate the DC bus current, the reference voltage of the DC bus is taken ($V_{DC} = 325\ V$), which it is supply the BLDC motor that was used in this investigation. The WPS and PV system desing in this thesis was done based on the parameters of the BLDC motor as shown in Table 3.3 which contains information on the specifications of the BLDC motor(Kumar and Singh 2016,p.2315-2322) .

$$I_{MP,total} = \frac{P_{MP,total}}{V_{MP,total}} = \frac{3600}{229.2} = 15.7\ A \tag{3.23}$$

$$N_S = \frac{V_{MP,total}}{V_{MP}} = \frac{229.2}{38.2} = 6 \tag{3.24}$$

$$N_P = \frac{I_{MP,total}}{I_{MP}} = \frac{15.7}{5.26} \approx 3 \tag{3.25}$$

$$D = \frac{V_{DC} - V_{MP,total}}{V_{DC}} = \frac{325 - 229.2}{325} = 0.3 \quad (3.26)$$

In this equation, D represents the duty cycle of the boost converter. The inductance of the boost converter can be calculated from the following equation (5)(Jena,Pudur, Ray, and Mohanty2019,p.200-205) .

$$L = \frac{V_{MP,total} \times D}{f_{sw}\, \Delta I_L} = \frac{229.2 \times 0.3}{20000 \times 15.7 \times 0.08} = 2.68 \approx 3\ mH \quad (3.27)$$

$$I_{DC} = \frac{P_{MP,total}}{V_{DC}} = \frac{3600}{325} = 11.07\ A \quad (3.28)$$

$$\omega = 2\,\pi\, f = \frac{2\pi\, N_r\, p}{120} = \frac{2 \times\ \pi\ \times 3000 \times 6}{120} = 942\,\frac{rad}{sec} \quad (3.29)$$

$$C = \frac{I_{DC}}{6 \times \omega \times \Delta V_{DC}} = \frac{11.07}{6 \times 942 \times 0.02 \times 325} = 301.3\ \mu F \quad (3.30)$$

The used capacitor in the simulation is 300 μF.

The water pumping constant is calculated from the following formula:

$$K = \frac{P}{{\omega_r}^3} = \frac{2890}{(2 \times \pi\ \times \frac{3000}{60})^{\,3}} = 9.3\ \times 10^{-5}\,\frac{W}{\frac{rad}{\text{sec}}^{\,3}} \quad (3.31)$$

Table 3.3 Technical parameters of the used BLDC motor

Parameter	**Value**
Rated Power, P	2890 W
Rated speed, N_r	3000 RPM
DC voltage, V_{DC}	325 V
Number of poles, p	6
Voltage constant, k_e	51 V_{LL}/K_{rpm}
Torque constant k_t	0.49 $N.m/A$
Phase to phase Stator inductance, R_S	0.36 Ω
Phase to phase stator Resistance, L_S	$1.3mH$

3.5. Design of battery energy storage system

Today, the technology of storage devices is employed to give electric power networks a high degree of stability and to provide the greatest performance possible for the issues that arise while employing renewable sources of energy(Yaqoob, Ferahtia , Obed, Rezk , Alwan, Zawbaa , Kamel 2022,p.63) . On the other hand, a number of states have recently passed laws that compel energy storage systems to increase the proportion of renewable energy that they absorb into their portfolios. These restrictions were enacted quite recently. These utilizations are seen to be extremely major challenges, and as a consequence, power conversion sources such as PV arrays need battery energy storage system (BESS) in order to meet their performance requirements(Ferahtia , Djeroui , Mesbahi , Houari , Zeghlache , Rezk , Paul 2021,p.1660)&(Thounthong, Pierfederici, Martin, Hinaje, Davat 2010,p.10).

When there was a decrease in the amount of solar irradiation, the BESS kind of lithium ion battery was used so that the performance of the WPS could be improved. In this scenario, the BESS will be the one to provide the WPS, and it will also be the one to facilitate the passage of power from the BESS to the BLDC motor while maintaining a reference voltage of 325 V at the DC bus. Figure 3.17 provides a visual representation of the BESS's block diagram that molded under MATLAB/Simulink. The following values for the battery's parameters are those that are utilized in this investigation:

- Battery voltage : **325 V**
- Battery size: **10 Ah**
- Initial SOC: **80 %**

Figure 3.18 illustrates the BESS's electrical properties used in this thesis.

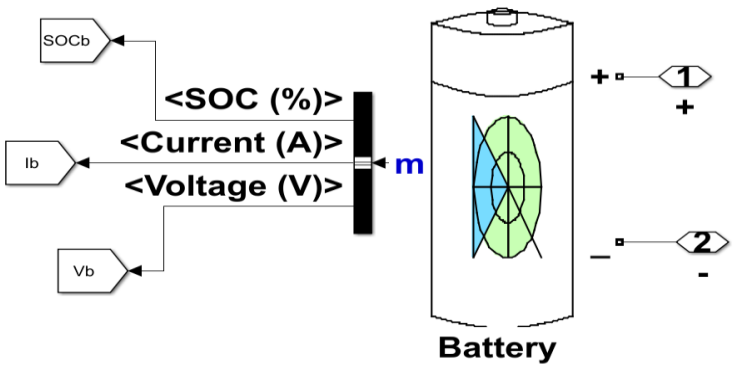

Figure 3.17 Block diagram of the BESS

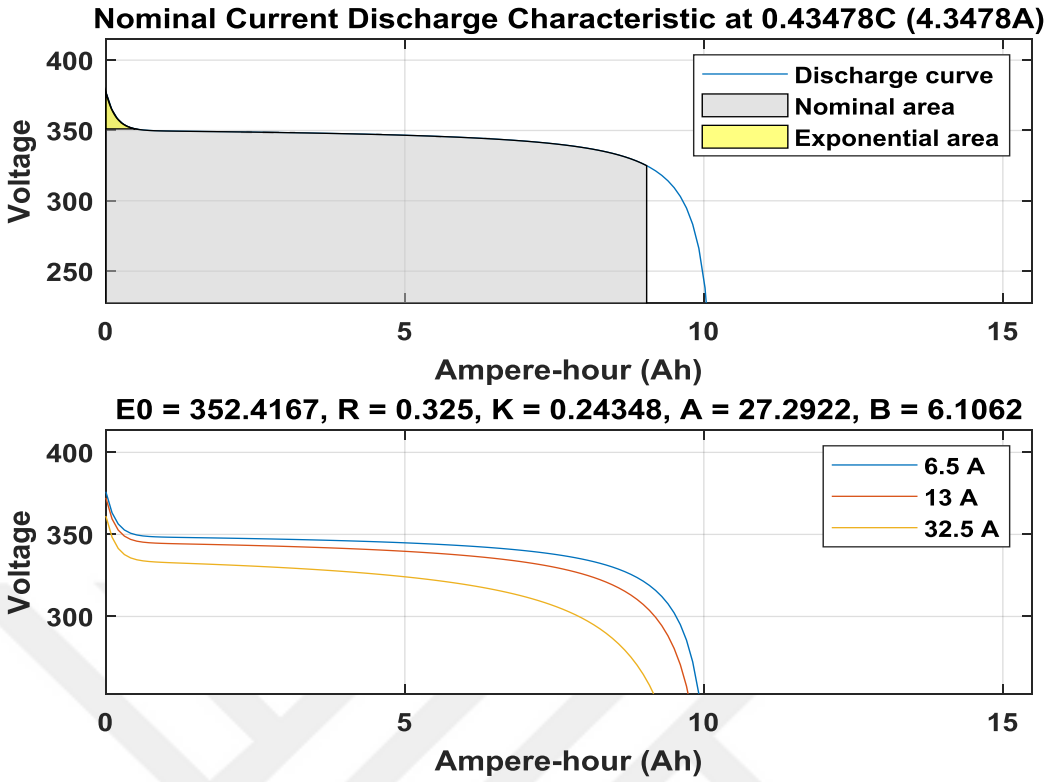

Figure 3.18 discharge characteristics of the battery

CHAPTER FOUR
RESULTS AND DISCUSSION

4.1 Introduction

In this chapter, the proposed MPPT method without using current sensor was proposed for the water pumping system powered by the PV system. The simulation of this thesis was done using MATLAB/Simulink software. The PV curves under different environmental conditions are presented, then the WPS is subjected to different values of irradiance and temperature profiles to study the dynamic performance of the BLDC motor under this climate conditions. To improve the functionality of the BLDC motor in a variety of climates, the suggested WPS based PVS incorporates battery energy storage. The proposed system has been demonstrated the viability and efficacy of the suggested strategy via simulation in the MATLAB/Simulink environment. It has been shown that the proposed MPPT would enhance the functionality of PV system-based battery charging in a variety of climates. The proposed method may converge more quickly, and it maintains a suitable steady state even if the surrounding circumstances change, as shown by a comparison with the classical P&O MPPT method.

4.2 MATLAB/Simulink Representation

Figure 4.1 shows the suggested PV systems for the WPS driven by BLDC motor. As seen, the proposed system structure consists of PV array with maximum power (3.6 KW), DC/DC boost converter, a single sensor MPPT controller, battery energy storage system (BESS), voltage source inverter (VSI), control unit of BLDC motor, BLDC motor, and water pump. The suggested model in MATLAB system was description in Fig.4.2.

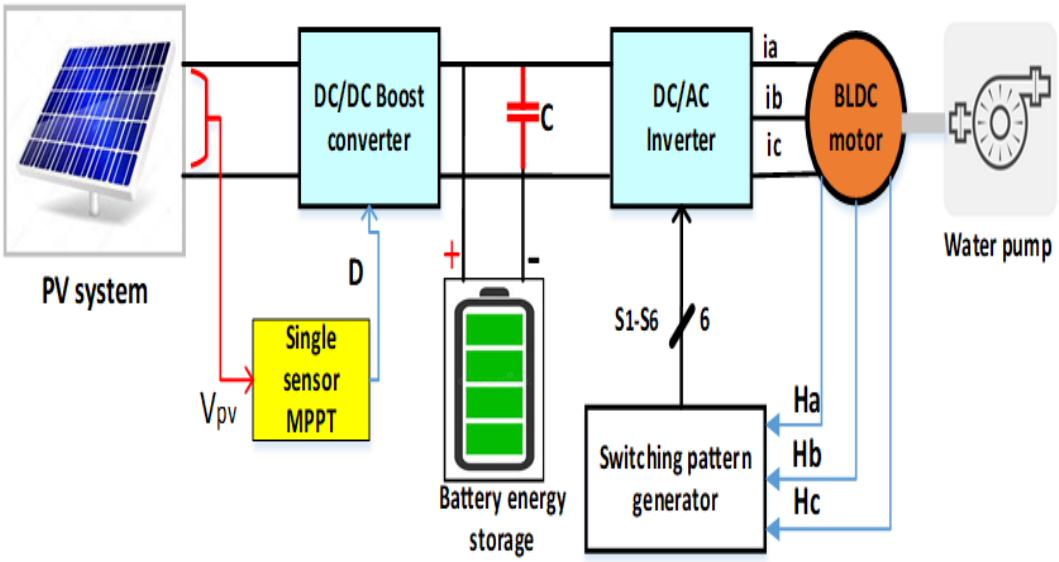

Figure 4.1 Proposed system configuration for WPS with current sensor-less MPPT

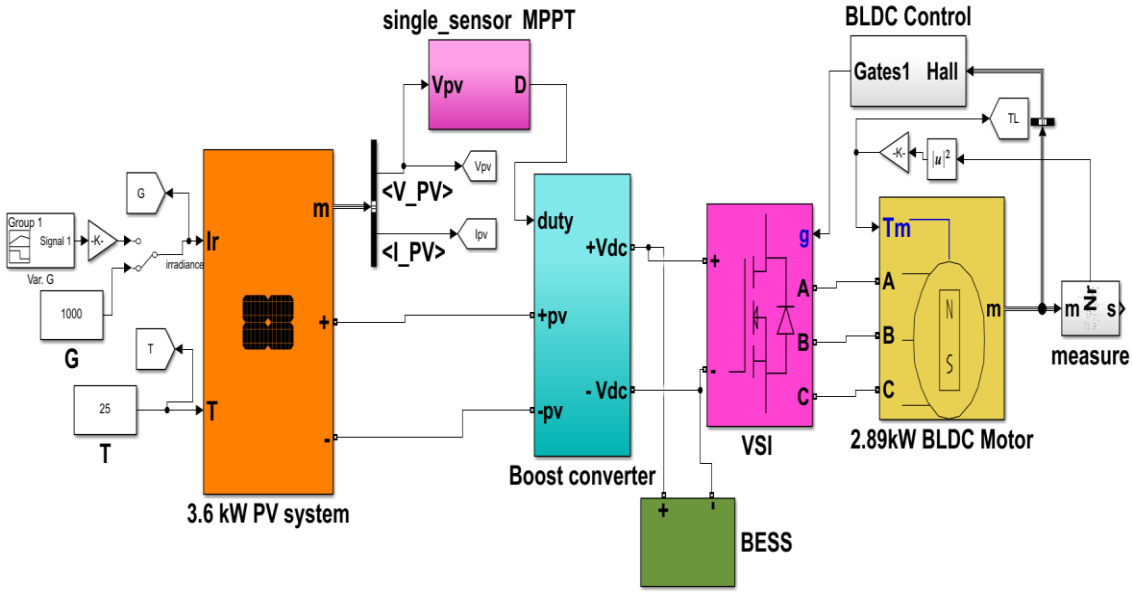

Figure 4.2 MATLAB/Simulink of the proposed WPS

To see the sub-system of the PV system Fig. 4.3 was used as seen to show the parameters of the PV array that molded in this thesis. Fig.4.4 show the boost converter circuit under MATLAB/Simulink. This circuit was designed in chapter three and the main parameters of this circuit was used here in MATLAB model. the suggested MPPT method used in this thesis was modelled in Simulink as presents in Fig.4.5.

The PWM generator was used to produce the required pulses for the switch based on the optimal value of the duty that generated from the MPPT controller.

Fig.4.6 presents the sub-system of the BLDC motor which has been model in this chapter. The type of the BLDC motor is trapezoidal back EMF waveform.

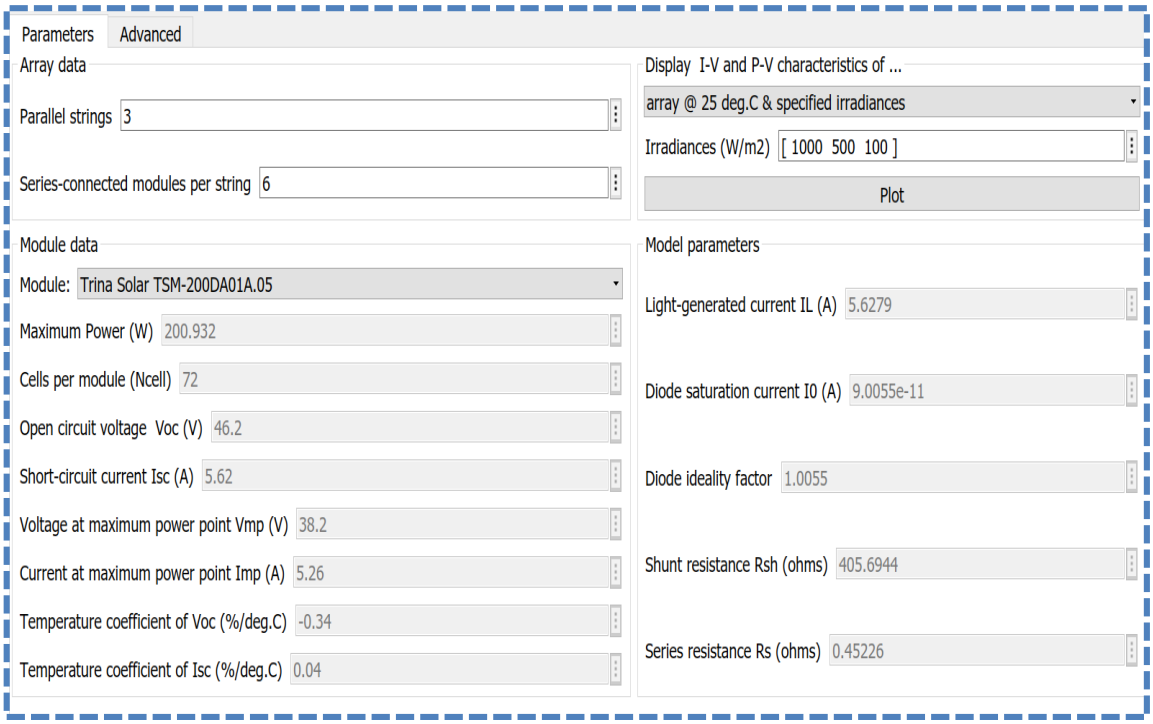

Figure 4.3. PV module /array parameters of TSM-200DA01A.05

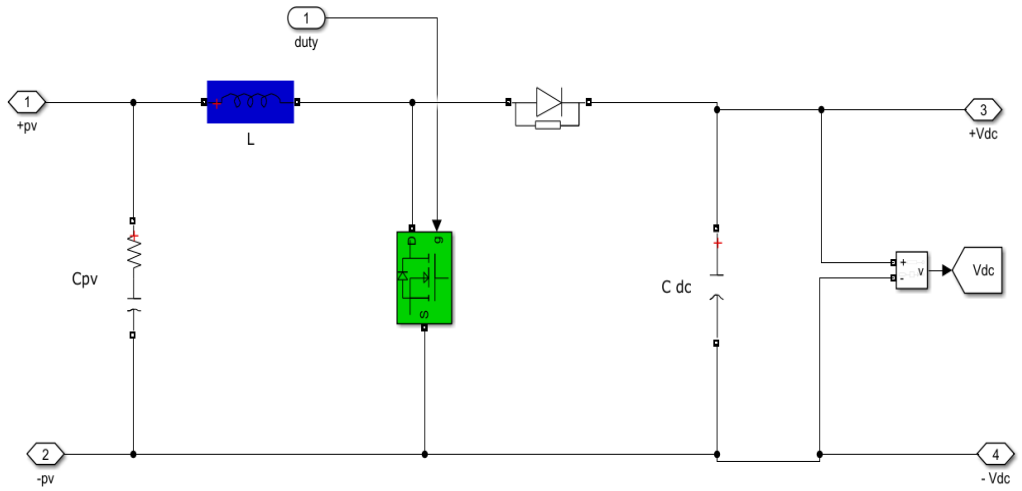

Figure 4.4. Model MATLAB of boost converter

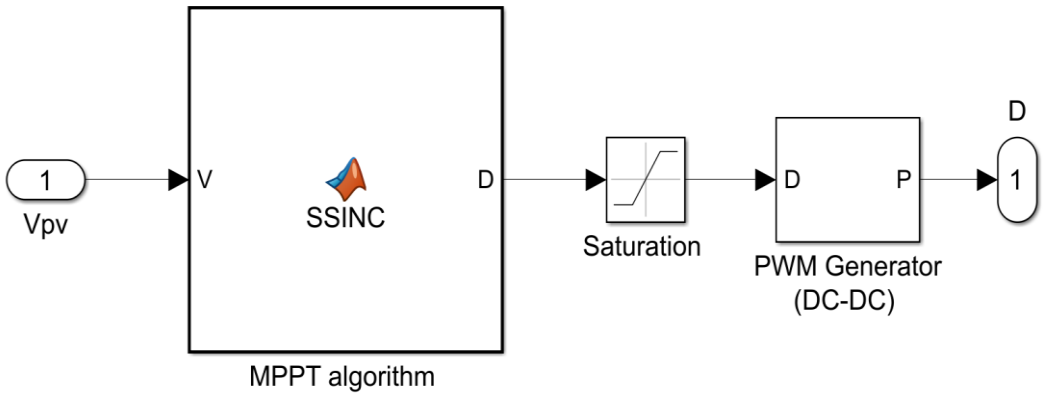

Figure 4.5. Model MATLAB of proposed MPPT algorithm

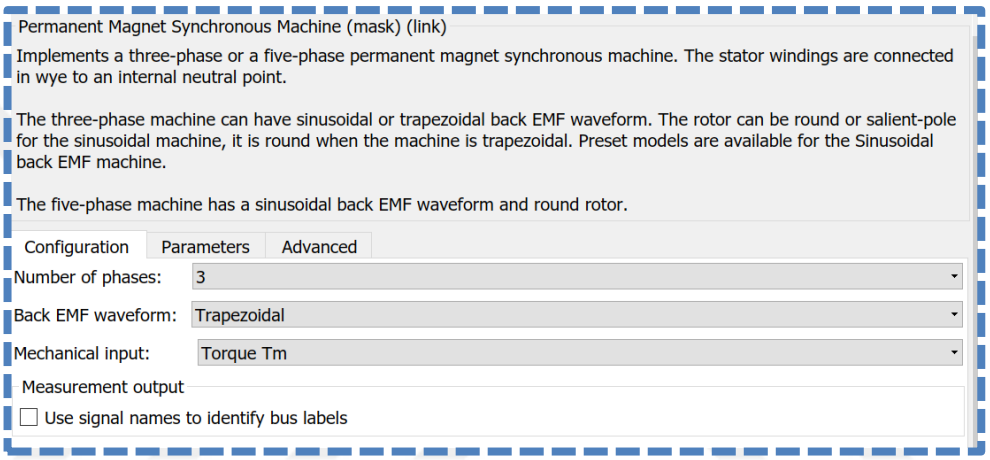

Figure 4.6 BLDC motor type used in this thesis.

Figure 4.7 show the control unit of the BLDC motor based electronic commutation method. As seen in this figure, the hall sensors for detect the position are used as input to generate the required back emf for the three phases using decoder sub-system. The model of the decoder was presented in Fig.4.8. The obtained gates for the VSI switches is presented in Fig.4.9. The true tables for the decoder and the gates are shown in Fig. 4.10

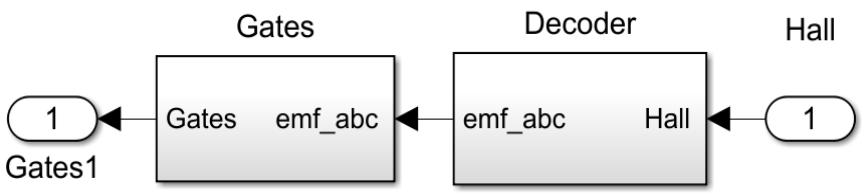

Figure 4.7. Control unit of the BLDC motor based electronic commutation control

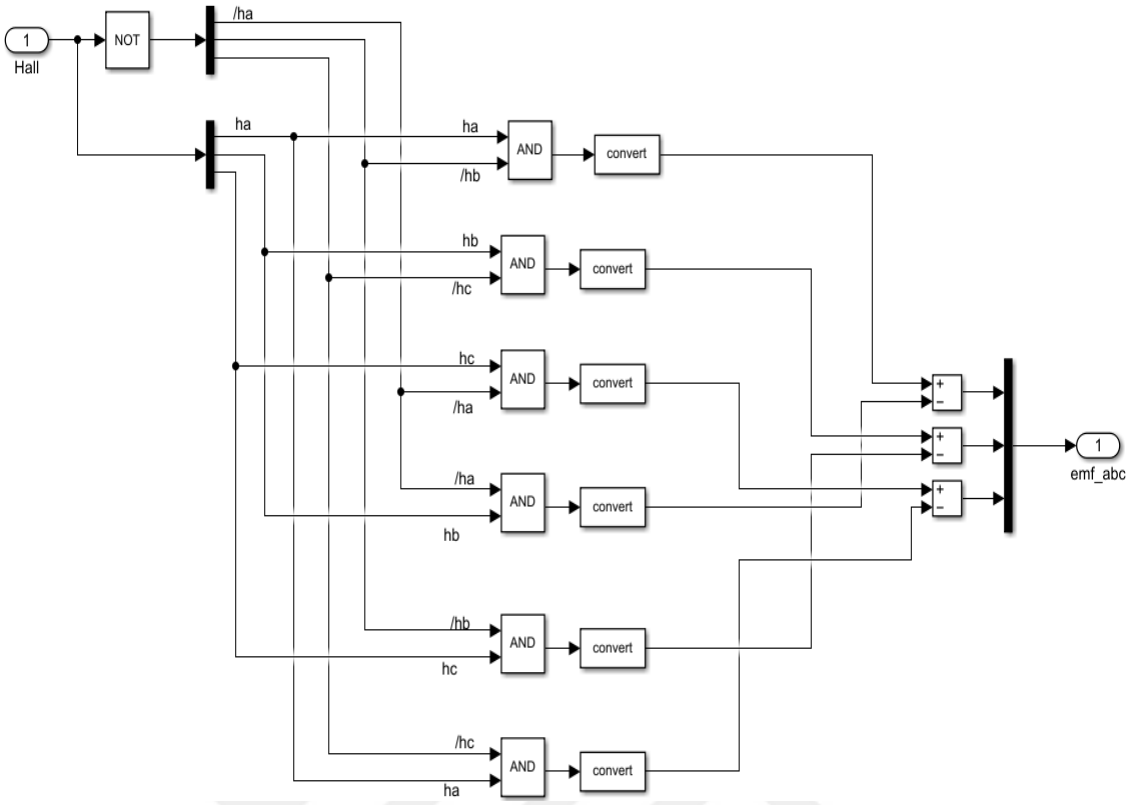

Figure 4.8 The sub-system model of the decoder

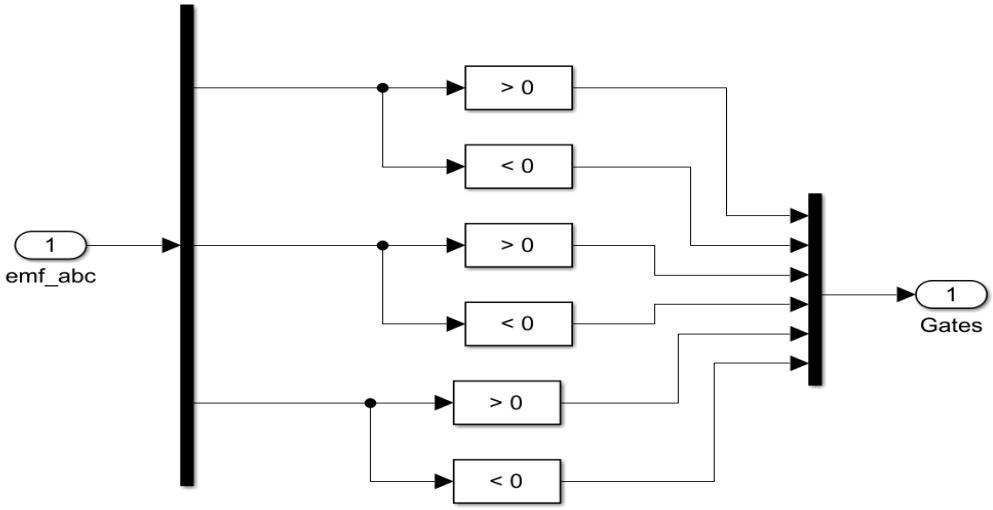

Figure 4.9 The sub-system model of the emf to gates control

the true table of Hall-emf module

ha	hb	hc	emf_a	emf_b	emf_c
0	0	0	0	0	0
0	0	1	0	-1	+1
0	1	0	-1	+1	0
0	1	1	-1	0	+1
1	0	0	+1	0	-1
1	0	1	+1	-1	0
1	1	0	0	+1	-1
1	1	1	0	0	0

(a)

The true table of emf-gates

emf_a	emf_b	emf_c	S1	S2	S3	S4	S5	S6
0	0	0	0	0	0	0	0	0
0	-1	+1	0	0	0	1	1	0
-1	+1	0	0	1	1	0	0	0
-1	0	+1	0	1	0	0	1	0
+1	0	-1	1	0	0	0	0	1
+1	-1	0	1	0	0	1	0	0
0	+1	-1	0	0	1	0	0	1
0	0	0	0	0	0	0	0	0

Figure 4.10 (a) true table of the decoder system (b) true table of the gates control

4.3 Simulation results and discussion

4.3.1 P-V and I-V characteristics of the PV array

In Figures 4.11 and 4.12, we can see the I-V and P-V characteristics of the 3.6 kW PV array that was employed in this investigation. Various levels of solar irradiation (1000 W/m^2, 500 W/m^2, and 250 W/m^2) and temperatures (25C^o) are used to evaluate the PV array, as shown in Fig.4.11. The photocurrent is very responsive to changes in irradiance value and has a significant impact on the PV array's power output. Moreover, if irradiance drops, the PV array's output voltage will fall small. As can be seen in Fig.4.11, the PV array's output current is relatively insensitive to changes in temperature, but the open-circuit voltage is significantly affected by rising temperatures because the temperature coefficient of the open-circuit voltage has a negative sign and thus causes a decrease in voltage as the temperature rises.

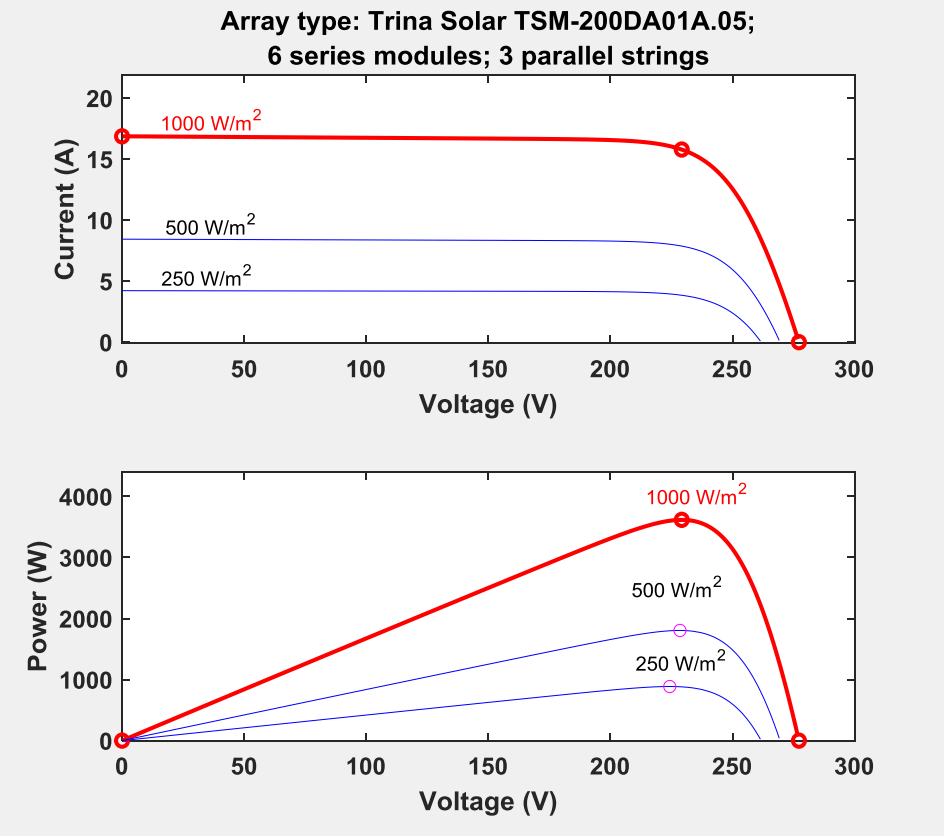

Figure 4.11 PV array curves under constant temperature and different irradiance levels

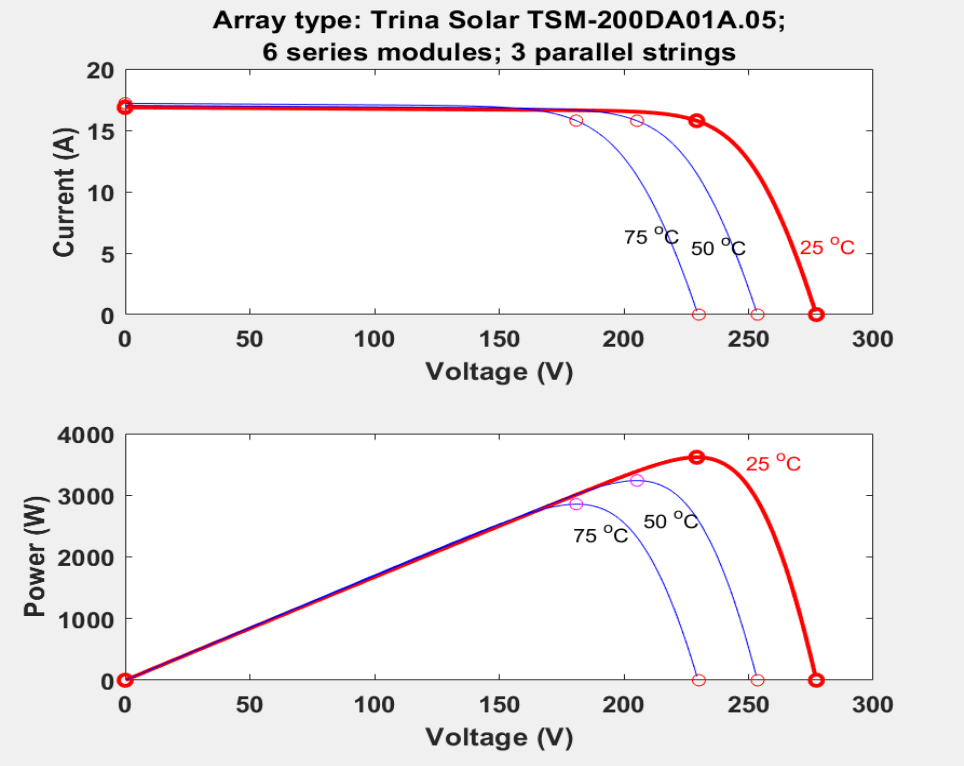

Figure 4.12 PV array curves under constant solar irradiance and different temperature values

4.3.2 Test performance of the WPS under constant weather conditions

Here, the suggested WPS was put through its paces under standard laboratory settings (G=1000W/m2 and T=25 C). Fig.4.13 shows the PV array results under constant weather conditions. The current, voltage and power are obtained for the simulation time of t=3 sec. It has been shown that the suggested MPPT controller can provide maximum power with little steady-state oscillation and a somewhat slow reaction time. Using an output current of 15.7 A and a PV voltage of 229 V, we can calculate the maximum power to be 3600 W. In contrast, the DC bus voltage and PV voltage are shown in Fig.4.14. As a result, the DC bus value produced here is 325 V, with little ripple and this is the main advantage of the proposed MPPT which is deliver a smooth DC voltage for the inverter and therefore the harmonic on the motor is less.

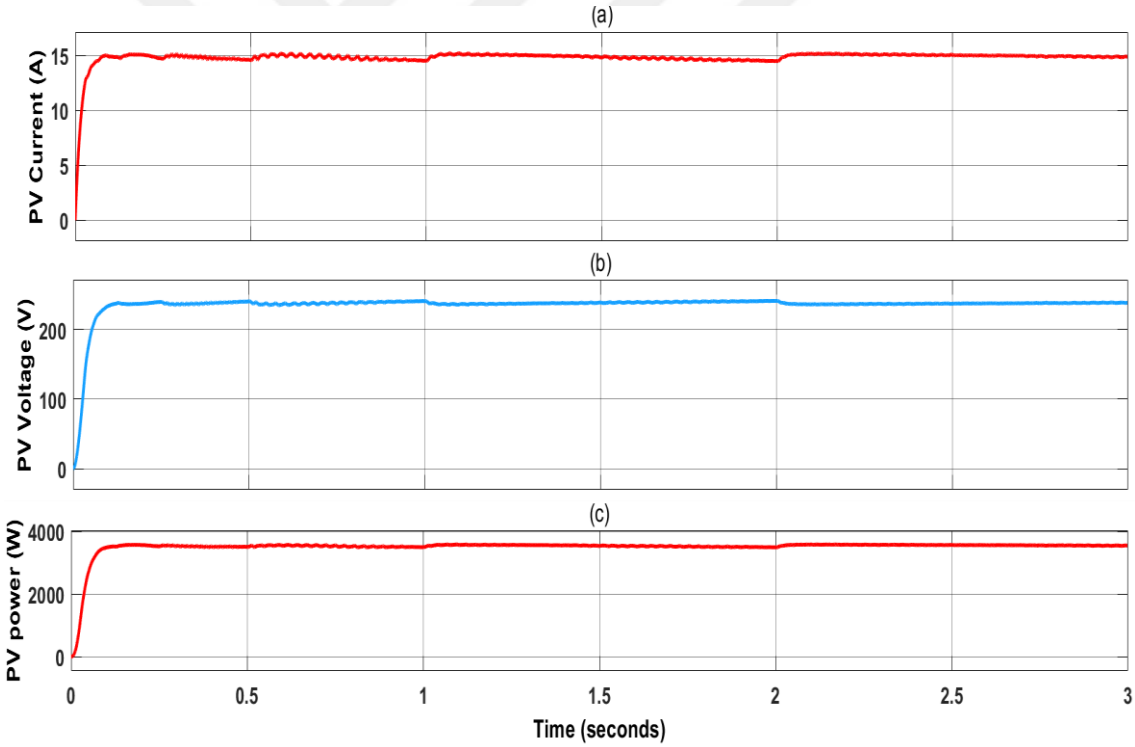

Figure 4.13 (a) PV current (b) PV voltage (c) PV power at STC conditions

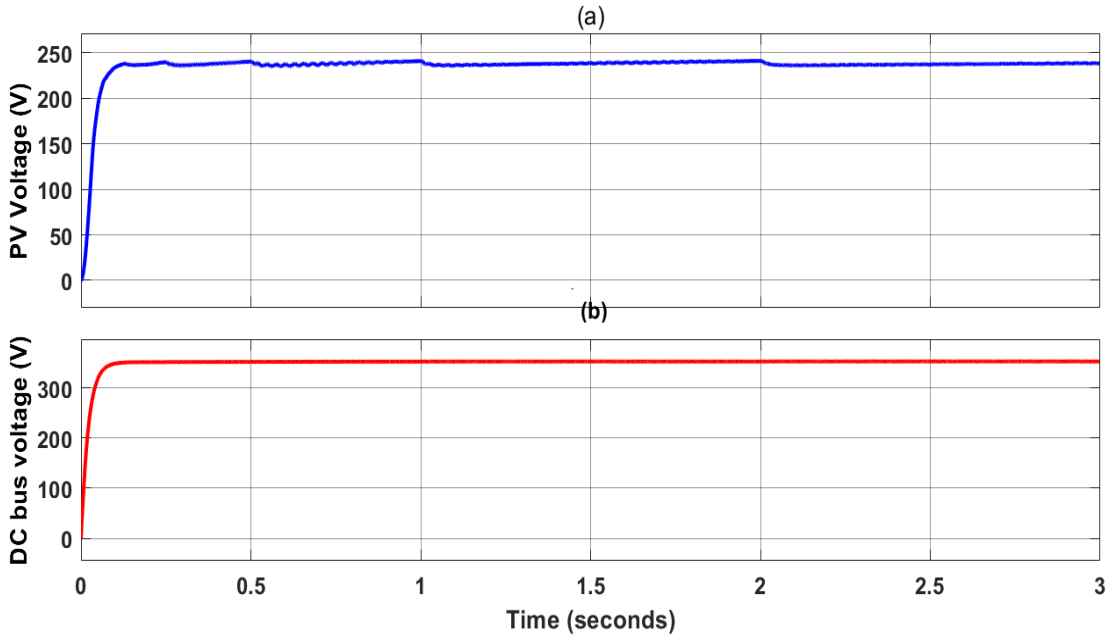

Figure 4.14 (a) output PV voltage (b) DC bus voltage

Fig.4.15 shows the outcomes of the BESS which are the voltage, current and SOC curves under constant weather conditions. These graphs show smooth results for the battery's voltage, current, and SOC with time while the weather stays the same. It can be seen from the curves that the BESS stays in charging mode while the solar PV array provides enough power for the WPS to function. The battery has a voltage of 325 V and a charging current of $I_b = -1.4\ A$ (note the negative value). The battery starts off with a SOC of 80%, and after being charged, it reaches a number greater than 80%.

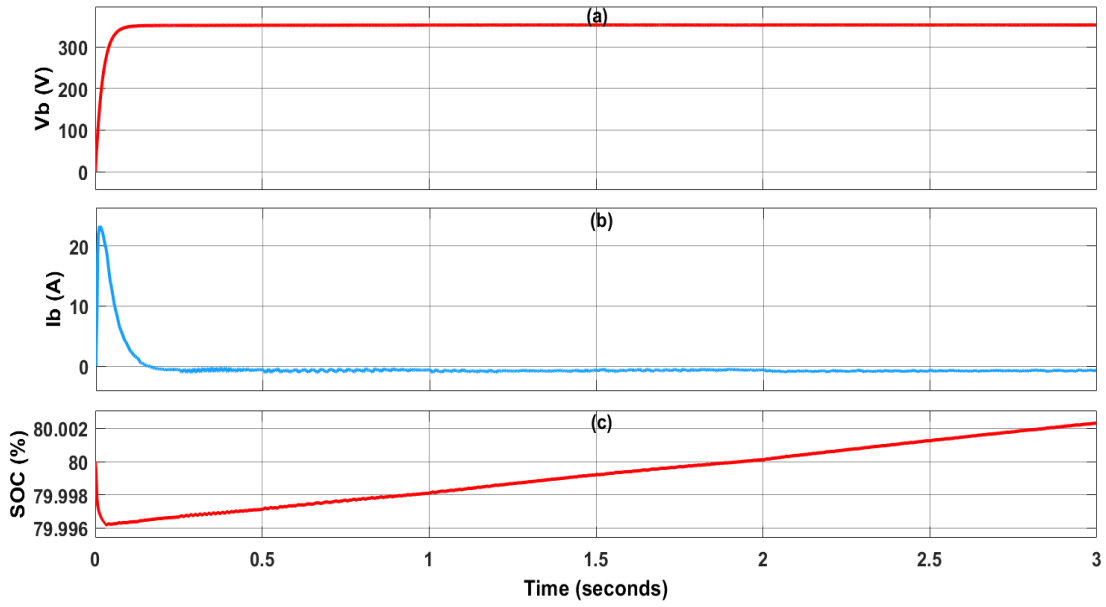

Figure 4.15 The BESS results under STC

BLDC motor output under STC circumstances are displayed in Fig.4.16. The back EMF for one phase is shown in Fig. 4.16(b), and the corresponding stator current (i_{sa}) is shown in Fig. 4.16 (a). The stator current at full load is $i_{sa} = 14.3\,A$, and $emf_{sa} = 163\,V$ as shown in the zoomed-in results of the BLDC's performance (Fig.4.17). Figure 4.18 illustrates the relationship between motor speed (N_r), electromagnetic torque (T_e), and the load torque (T_L) at rated motor conditions. These motor characteristics are measured under steady-state circumstances at full rated load. The motor-pump also starts and operates without any problems, demonstrating the effectiveness of the proposed setup. However, the BLDC motor's electronic commutation causes a little pulsation in T_e as seen in Fig.16. the rated speed of the motor is $3000\,rpm$ at load torque of $T_L = 10\,N.m$.

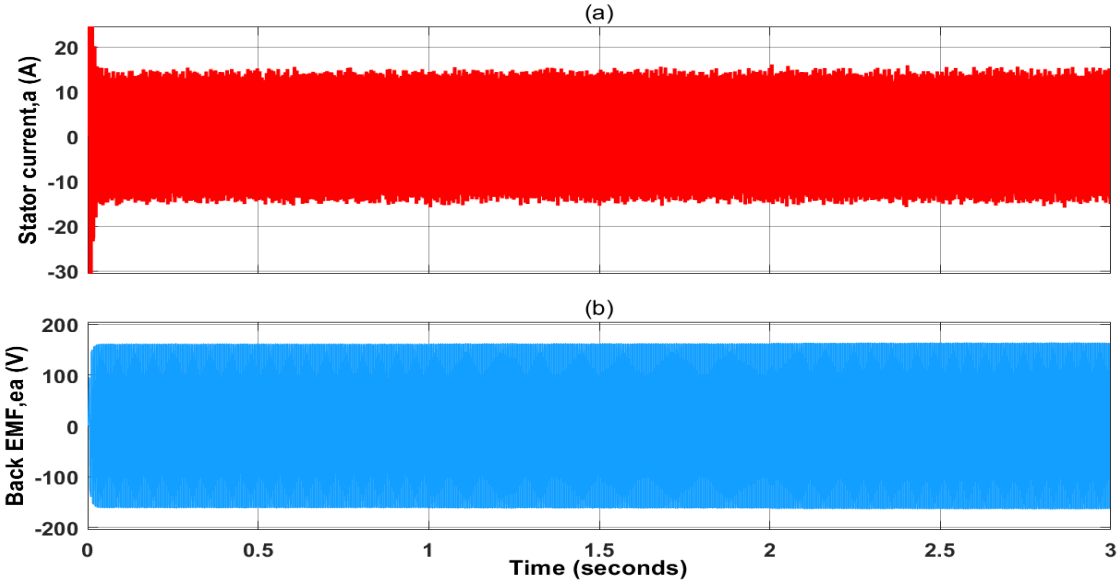

Figure 4.16 performance of the BLDC motor under STC conditions (a) stator current for phase a (b) back EMF for phase a.

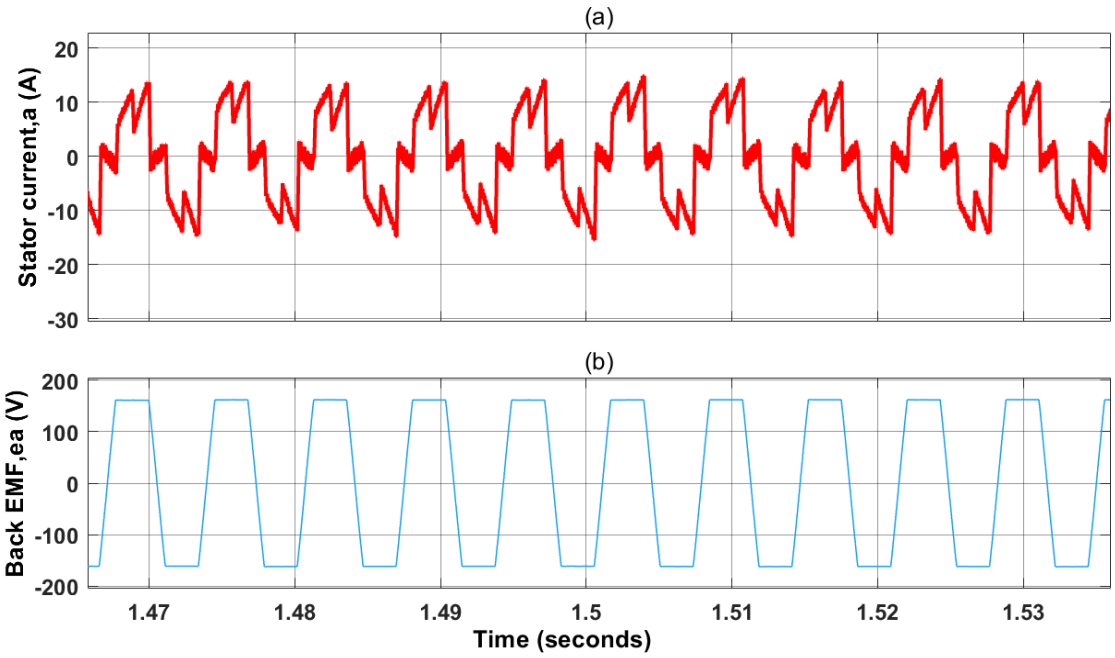

Figure 4.17 zoom results of emf and Isa.

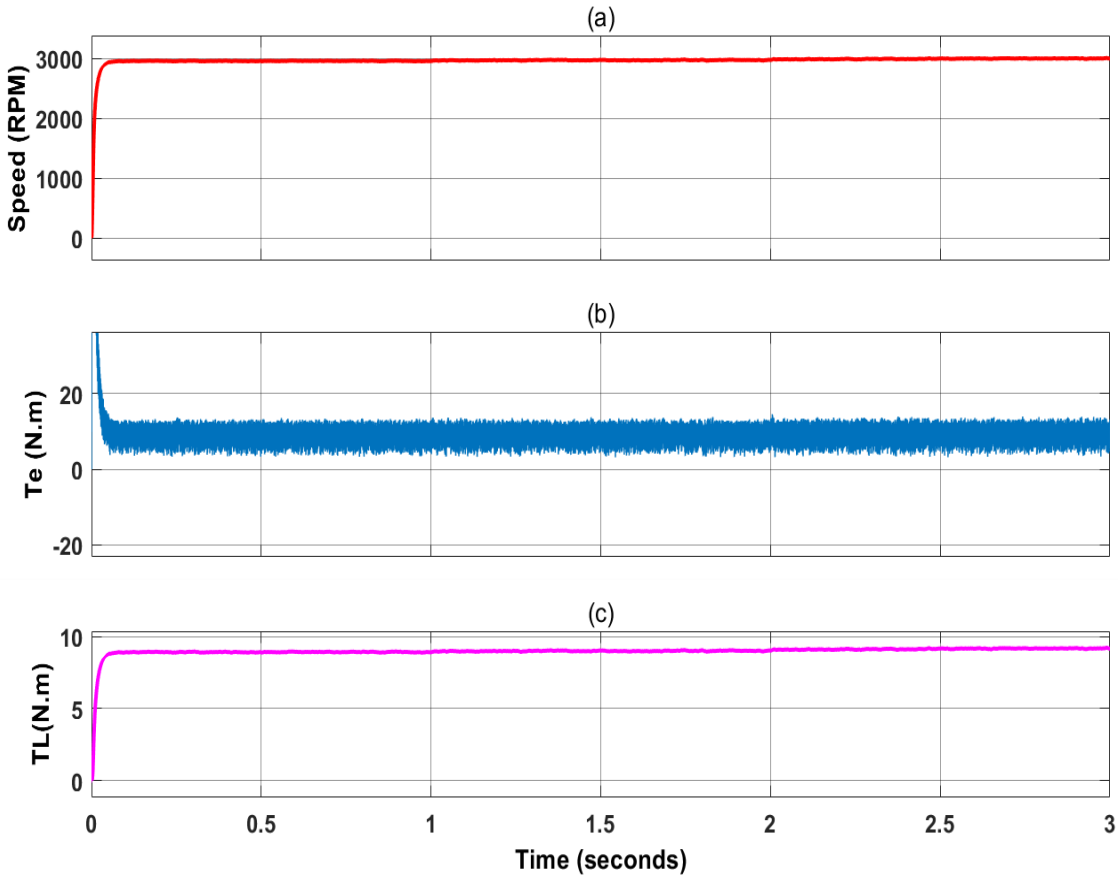

Figure 4.18 the performance of the BLDC motor under STC conditions (a) speed of the motor in RPM (b) electromagnetic torque in N.m (c) applied load or load torque

Fig.4.19 show the three phase stator currents of the BLDC motor $(i_{sa}, i_{sb}$ and $i_{sc})$ at steady state operation. Fig.4.20 show the 3- phase back EMF of the BLDC motor $(e_a, e_b$ and $e_c)$ at steady state case. Fig.4.21 shows the hall signals of the BLDC motor position for the time interval from t=1.38 sec to 1.45 sec.

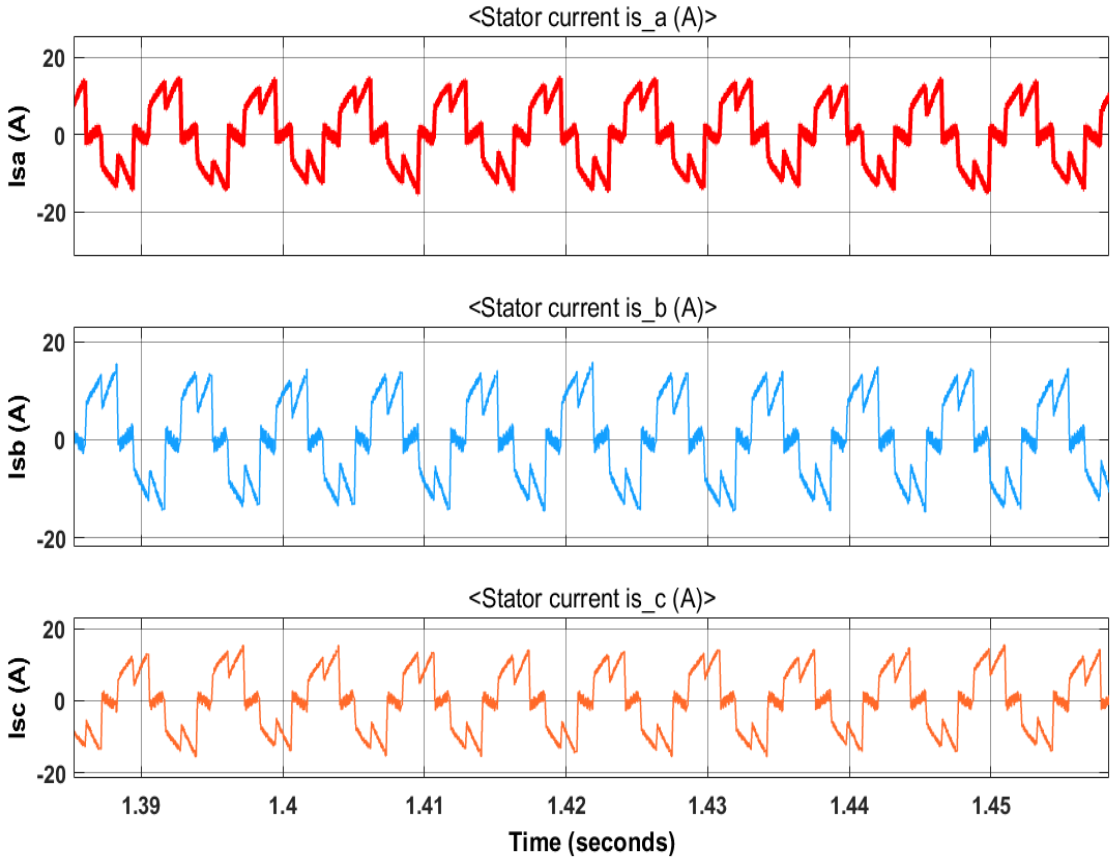

Figure 4.19 the three phase stator currents of the BLDC motor $(i_{sa}, i_{sb}$ and $i_{sc})$ at steady state operation.

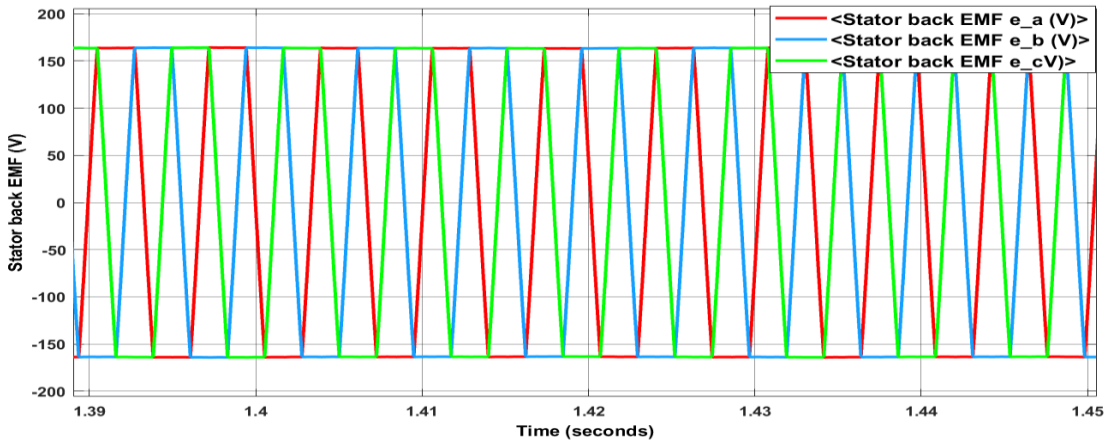

Figure 4.20 the 3- phase back EMF of the BLDC motor $(e_a, e_b$ and $e_c)$ at steady state case

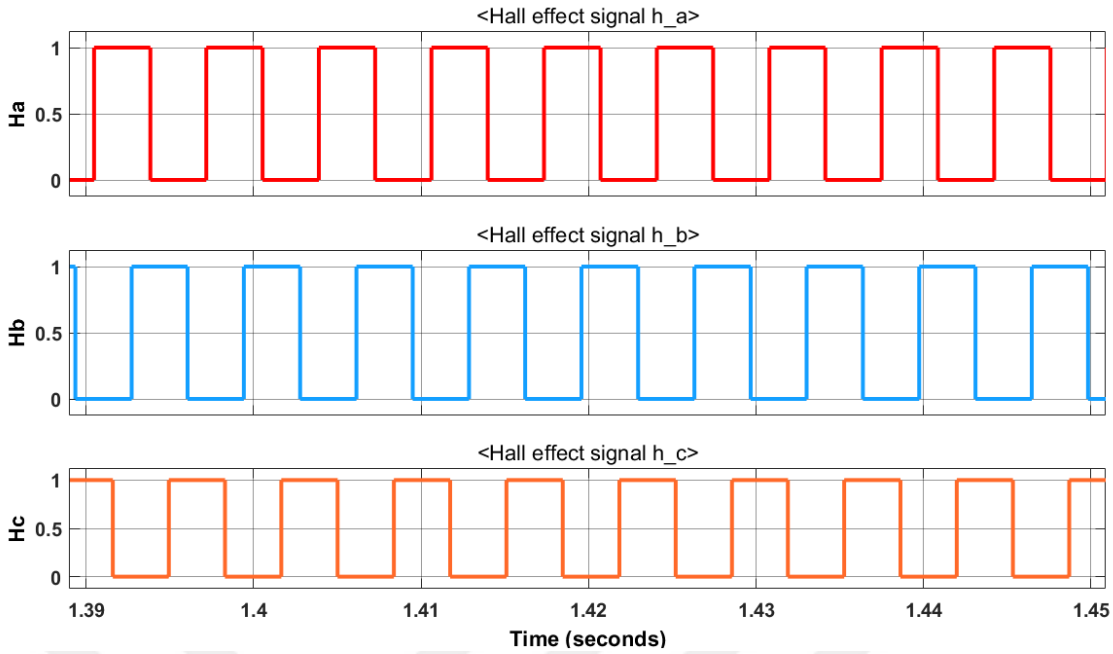

Figure 4.21 the hall signals of the BLDC motor position

4.3.3 Test performance of the WPS under variable weather conditions

Here, at a constant temperature of 25 degrees Celsius, the performance of the PV system and the BLDC motor are assessed under a range of irradiance conditions. In this simulation, the weather conditions are changed for the solar irradiance curve from 250 W/m^2 to 500 W/m^2 to 1000 W/m^2 as shown in Fig.4.22. Figure 4.23 displays the data collected from the PV array. It is clear that, the amount of the power harvested by the PV modules is reduced proportional to the solar irradiance level.

As result, this reduction cause reduction in the voltage and current that supplied the BLDC motor and may cause reduction in its speed. In this thesis, the BESS was used to avoid this problem as shown in Fig.4.24. In this curve, the power generation from the PV array at time interval 0 sec to 1 sec is very low and therefore the BESS has been supplied the BLDC motor. moreover, the BESS is supplied the required load by $P_b = 2400\ W$ or WPS form time t=0 sec to t=1 sec due to the irradiances value in this interval is G=250 W/m², and it supplied the BLDC motor by $P_b = 1450\ W$ due to the irradiance value in this (1 sec to 2 sec) interval is G=500 W/m². Also, the power of the PV array at third interval is high and therefore the BESS was converted from the discharging to the charging mode and then battery's power become in negative sign of $P_b = -400\ W$. The maximum power at G=250 W/m² is $P_{MP} = 875W$, and it is equals

$P_{MP} = 1800\ W$ at G=500 W/m² and the PV power at highest value of $P_{MP} = 3600\ W$ at G=1000 W/m². The BESS makes the voltage is constant through the reduction in irradiance and the power flow will pass from battery to the motor as shown in Fig.4.25.

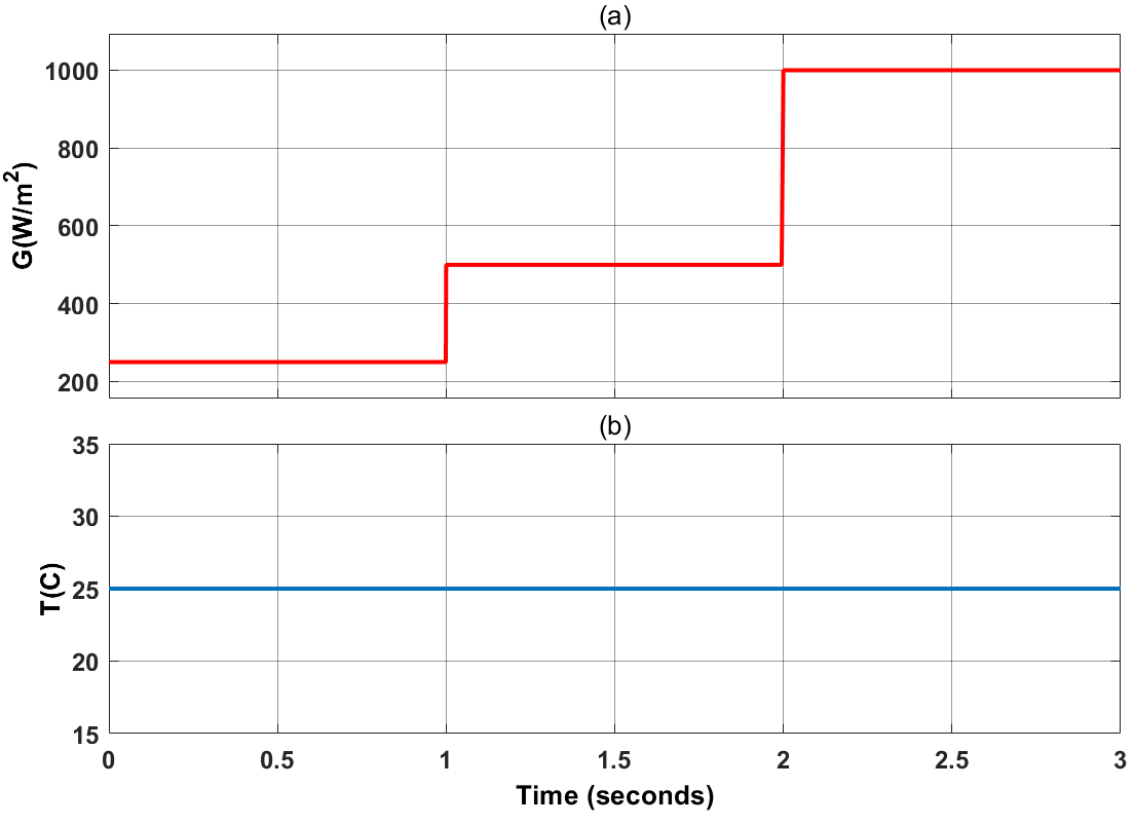

Figure 4.22 the simulated profile for the temperature and irradiance

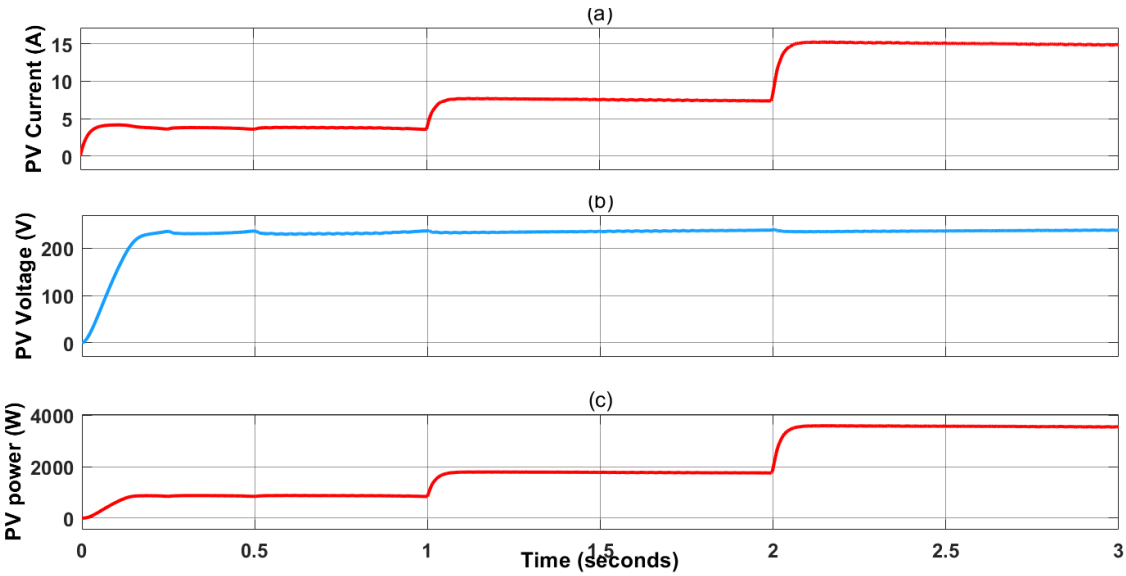

Figure 4.23 obtained results of the PVS under various levels of irradiation

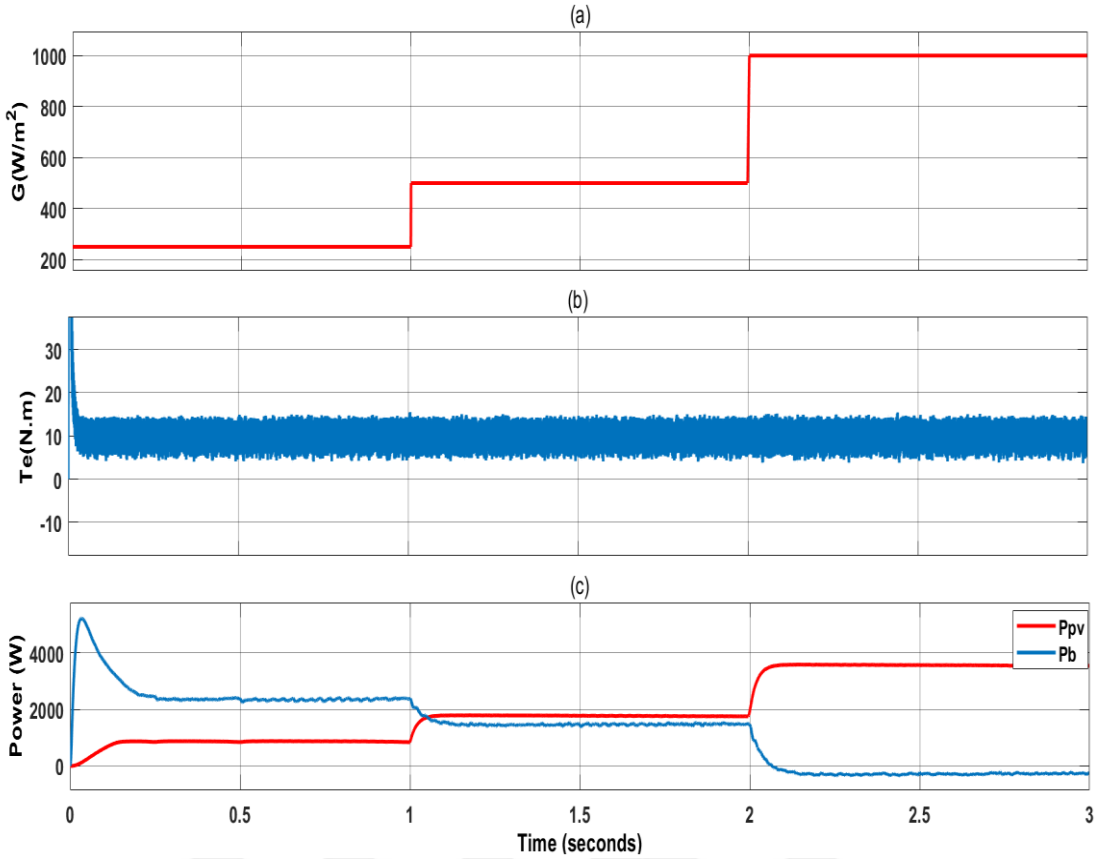

Figure 4.24 (a) irradiance levels (b) electromagnetic torque (c) output power of the PVS and BESS

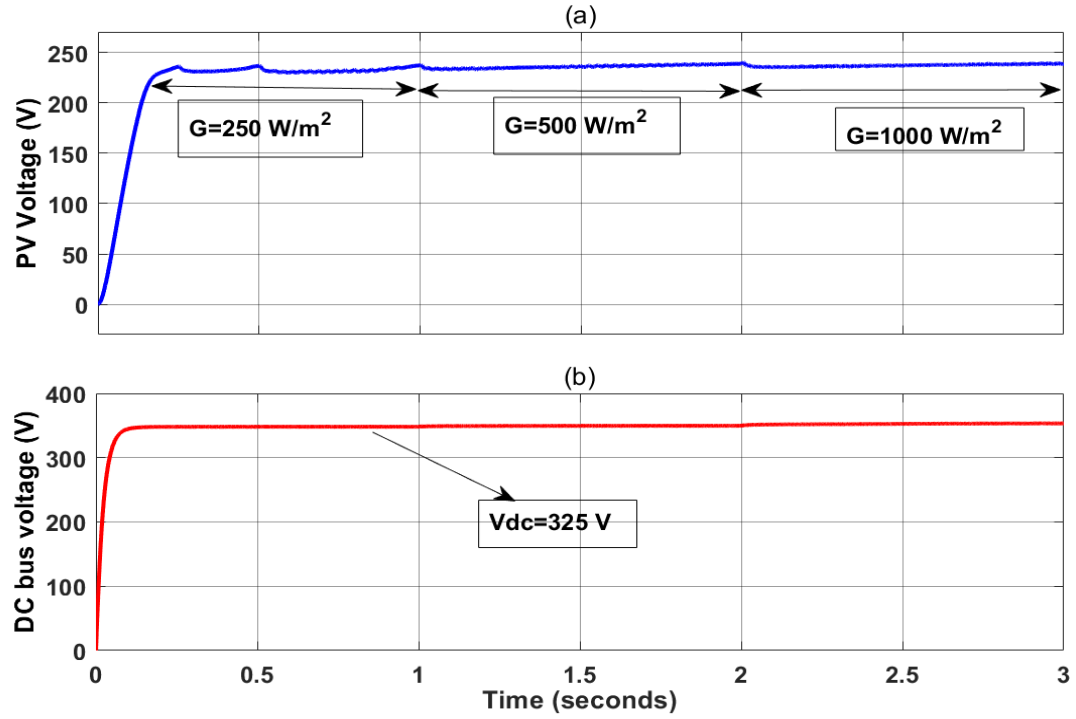

Figure 4.25 (a) PV voltage (b) DC link voltage

The BLDC motor can reliably reach speeds greater than 2950 rpm, the minimum speed needed to pump water at an irradiance of 250 W/m^2. The BLDC motor's efficiency does not drop in bad weather, and it can effectively pump water as seen in Fig.4.26. This feature of the using BESS which is makes the DC voltage is constant at 325V and therefore it keeps the speed of the motor is constant approximately.

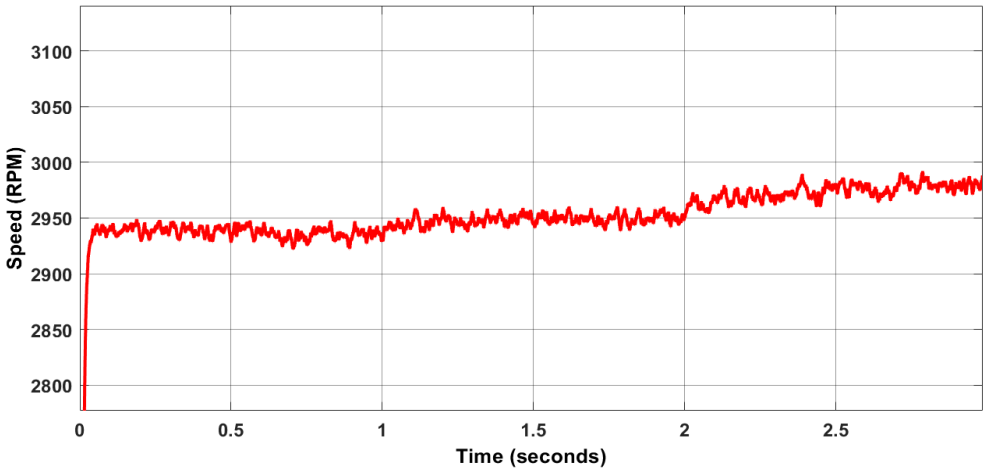

Figure 4.26 speed of the BLDC motor at varying irradiance

4.3.4 Comparison between the proposed and P&O based MPPT methods

To clear the novelty of this work, a comparison between the recommended MPPT method and the classical P&O method under various values of irradiance was presented as seen in Figs.(4.27-4.29). It is clear that, the suggested MPPT method is more accurate faster than the conventional method. Also, the smooth curve of the PV array indicate that the proposed MPPT is more efficient than the conventional method and it is has high efficiency with less power oscillation around the MPP. moreover, the solar irradiance and temperature profile that has been presented in Fig.4.22 was used in this comparison. The voltage, current and power curves of the PV system under the proposed MPPT method are more smooth and accurate against the curves of the classical P&O method.

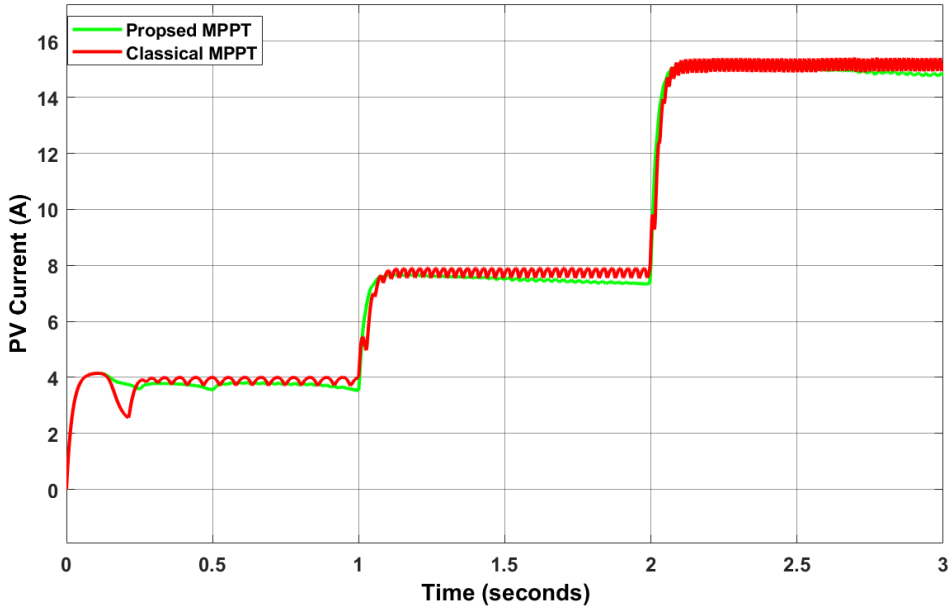

Figure 4.27 PV current results of the PVS under classical MPPT method and proposed MPPT method at constant temperature and step changes in irradiance

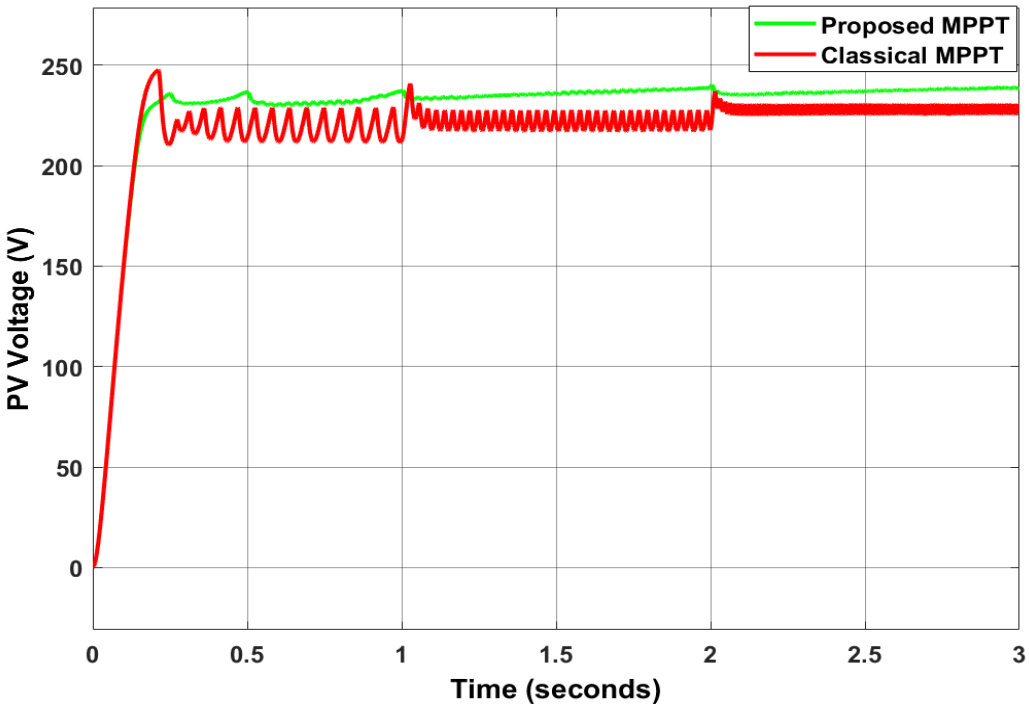

Figure 4.28 PV voltage results of the PVS under classical and proposed MPPT methods at constant temperature and step changes in irradiance

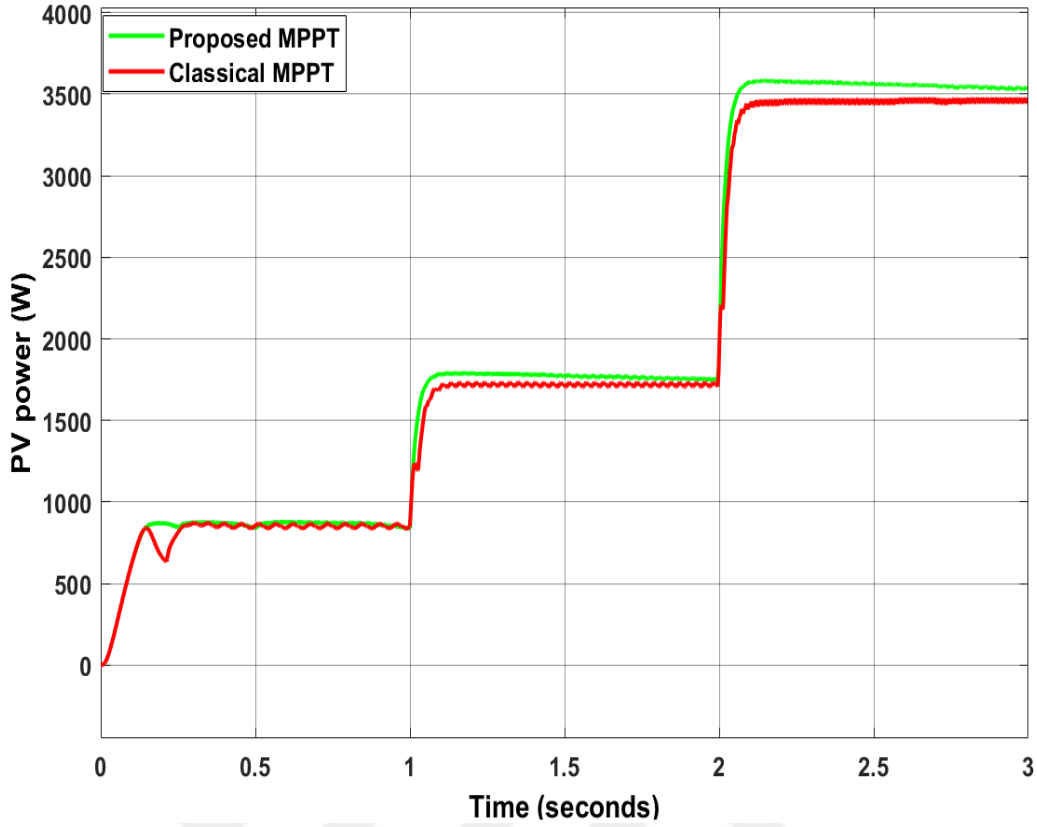

Figure 4.29 PV power results of the PVS under classical and proposed MPPT methods at constant temperature and step changes in irradiance

Above shown above, the suggested technique for the MPPT controller offers improvements over prior approaches, including lower power oscillation, lower ripple content, a better dynamic response, and increased efficiency. In addition, the new single-sensor approach demonstrated reduced effect from both issues when solar irradiation went from low to high or vice versa, while the conventional P&O method suffered from both. In cases when the irradiance is rapidly changing, the suggested MPPT approach provides accurate results that show a more steady PV power with a decreased ripple content.

Furthermore, the effect of the varying temperature on the performance of the PV modules has been studied in this discussion. For this reason, this effect was done in simulation by decreasing the value of the temperature as shown in Fig.4.30. The solar irradiation keeps constant at 1000 W/m^2.

The results obtained in this conditions are displayed in Figs.(4.31-4.33). when T is varied from 25C to 0C, the amounts current and voltage are increased cause increasing in the output power for the PV modules. The archived results using

suggested MPPT are more accurate and less oscillation when compared that the classical method.

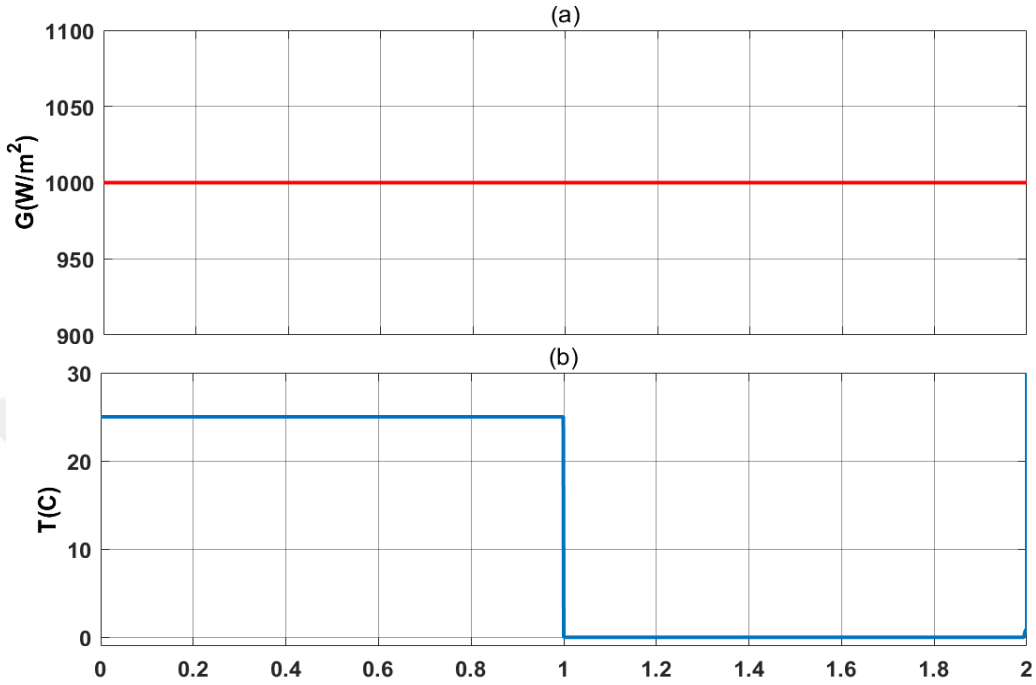

Figure 4.30 weather conditions profile

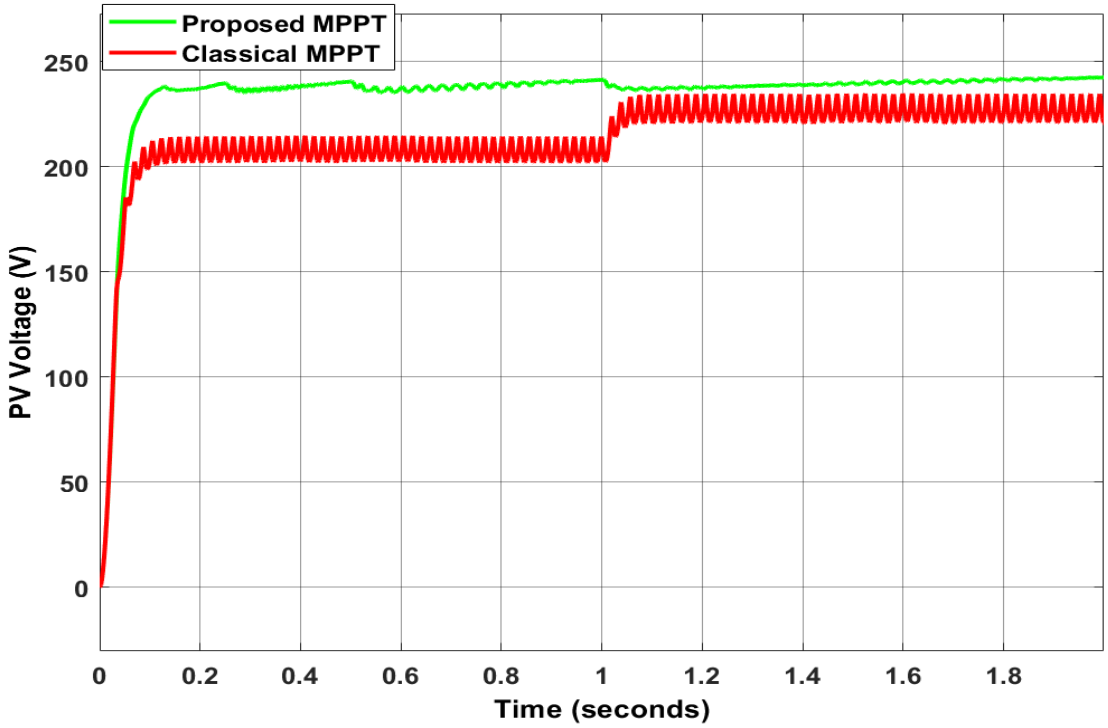

Figure 4.31 PV current results at constant irradiance and step changes in temperature

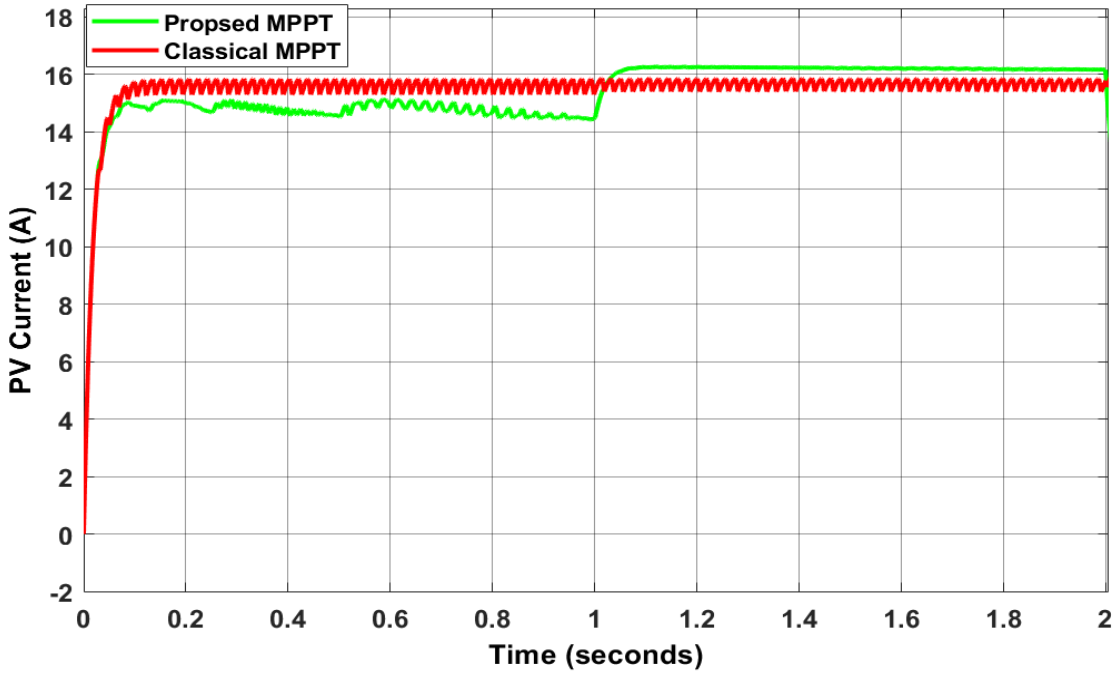

Figure 4.32 PV current results at constant irradiance and step changes in temperature

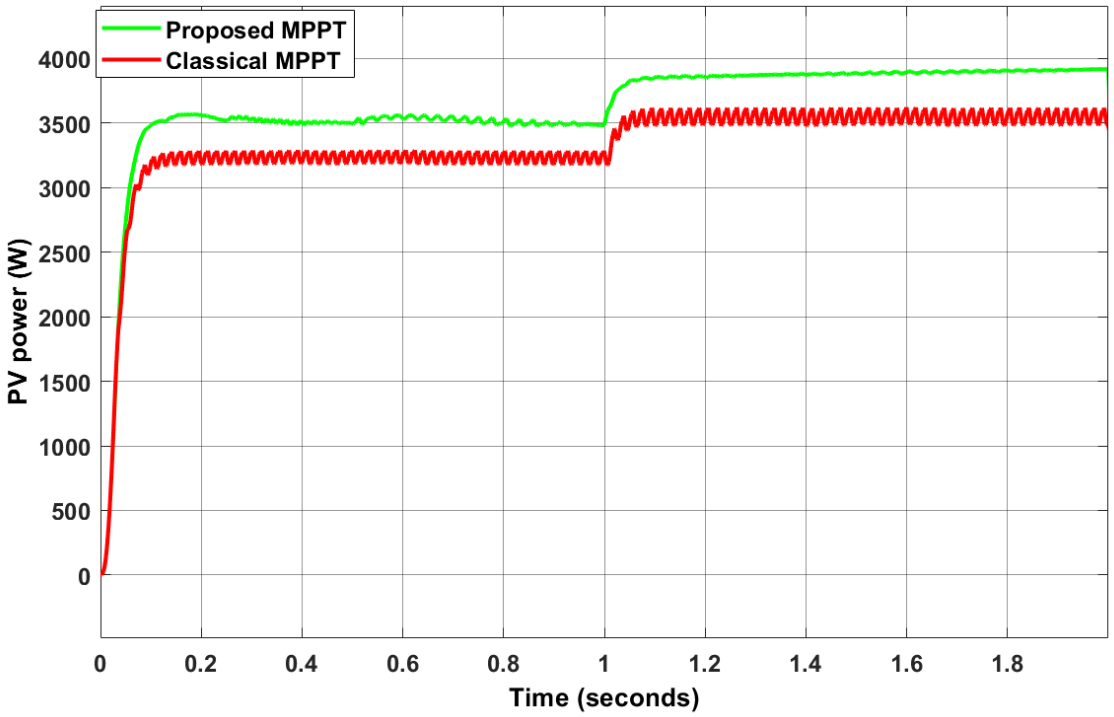

Figure 4.33 PV power results at constant irradiance and step changes in temperature

In summary, a low cost and simple MPPT method that only requires one sensor and can derive the greatest amount of power is presented in this thesis. The control circuit for the PV system is cheaper since the recommended technique did not need the expensive current sensor. As it turns out, when compared to the standard P&O MPPT, the proposed method shows promise for faster convergence and better steady-state performance across a range of environmental circumstances. Finally, compared to the conventional approach's 95.4% tracking efficiency, the new MPPT method showed 99.6%.

CONCLUSION

This thesis presents a low cost and simple MPPT approach that can extract the maximum amount of power from the PV system using only one sensor. In addition, this method only requires one sensor for the voltage of the PV and the circuit configuration is deigned without needing the current sensor. The proposed MPPT is implemented on the photovoltaic system that drives the brushless DC motor for the water pumping system (WPS). In order to improve the BLDC motor's overall performance in a variety of climatic circumstances, we suggested WPS-based PVS has energy storage in the form of batteries incorporated into it. The size of the PV system used here is 3.6KW which is used to power the WPS driven by 2.89 KW & 3000 RPM BLDC Motor.

The suggested technique was validated to demonstrate that it is both practicable and effective via the use of simulation in the environment provided by MATLAB and Simulink. Since the high-priced current sensor was not included in the design of the approach that was recommended, the cost of the control circuit that is responsible for the battery charging was lowered. It has been shown that the proposed MPPT will lead to an improvement in the performance of the PV system-based battery charging in a variety of climatic environments. In point of fact, the comparison with the traditional P&O MPPT shows that the suggested method may converge more quickly, and that it keeps a satisfactory steady state even if the environmental conditions change. This was demonstrated by the fact that it maintains a satisfactory steady state in the event that the environmental conditions change.

SCOPE FOR FUTURE WORKS

Suggestions that can be use to update and advance this thesis. To summarize, the following are some proposals for future works:

1. This thesis presented a WPS powered by PV system controlled by simple and low cost MPPT method. The robust MPPT control method such as grey wolf optimization (GWO), Salp swarm optimization (SSA), and artificial intelligent techniques will use to enhance the system performance and improve the efficiency.
2. Design and implement of a prototype of a single sensor MPPT method based Arduino microcontroller in hardware.
3. Design a real time control of the BLDC motor driven WPS for renewable energy sources.
4. Design a robust speed control method for the BLDC motor to enhance its performance under different load conditions.

REFERENCES

Abbas, Furqan A., Adel A. Obed, Mohammed A. Qasim, Salam J. Yaqoob, and Seydali Ferahtia. "An efficient energy-management strategy for a DC microgrid powered by a photovoltaic/fuel cell/battery/supercapacitor." *Clean Energy* 6, no. 6 (2022): 827-839.

Alkahtani, Mohammed, Zuyu Wu, Colin Sokol Kuka, Muflah S. Alahammad, and Kai Ni. "A Novel PV array reconfiguration algorithm approach to optimising power generation across non-uniformly aged PV arrays by merely repositioning." *J* 3, no. 1 (2020): 5.

Baimel, D., Tapuchi, S., Levron, Y., & Belikov, J. "Improved fractional open circuit voltage MPPT methods for PV systems" *Electronics*, vol.*8*, no.3. 2019.

Benzaouia, Mohammed, Loubna Bouselham, Bekkay Hajji, Anne Migan Dubois, Anas Benslimane, and Mostafa El Ouariachi. "Design and performance analysis of a photovoltaic water pumping system based on DC-DC boost converter and BLDC motor." In *2019 7th International Renewable and Sustainable Energy Conference (IRSEC)*, pp. 1-6. IEEE, 2019.

C. Urayai and G. A. J. Amaratunga, "Single-sensor maximum power point tracking algorithms," *IET Renewable Power Generation*, vol. 7, no. 1, pp. 82–88, Jan. 2013, doi: 10.1049/iet-rpg.2011.0264.

Dadkhah, J., & Niroomand, M. (2021). Optimization methods of MPPT parameters for PV systems: Review, classification, and comparison. *Journal of Modern Power Systems and Clean Energy*, *9*(2), 225-236.

Ferahtia S, Djeroui A, Mesbahi T, Houari A, Zeghlache S, Rezk H, Paul T. Optimal adaptive gain LQR-based energy management strategy for battery–supercapacitor hybrid power system. Energies. 2021 Mar 17;14(6):1660.

Gupta, Ankit, Pawan Kumar, Rupendra Kumar Pachauri, and Yogesh K. Chauhan. "Performance analysis of neural network and fuzzy logic based MPPT techniques for solar PV systems." In *2014 6th IEEE power India international conference (PIICON)*, pp. 1-6. IEEE, 2014.

Jately, V., Azzopardi, B., Joshi, J., Sharma, A., & Arora, S. "Experimental Analysis of hill-climbing MPPT algorithms under low irradiance levels" *Renewable and Sustainable Energy Reviews*, no.*150*, 111467. 2021.

Jain, K., Gupta, M., & Bohre, A. K. (2018, December). Implementation and comparative analysis of P&O and INC MPPT method for PV system. In *2018 8th IEEE India International Conference on Power Electronics (IICPE)* (pp. 1-6). IEEE.

J. Park, M. G. Jeong, J. G. Kang, and C. Yoo, “Solar Energy-Harvesting Buck-Boost Converter with Battery-Charging and Battery-Assisted Modes,” *IEEE Transactions on Industrial Electronics*, vol. 68, no. 3, 2021, doi: 10.1109/TIE.2020.2975491. [41

K. Uchihashi and H. Miyai, “Solar Powered Battery Charging Station,” *ASEE 2014 Zone I Conference, April 3-5, 2014, University of Bridgeport, Bridgpeort, CT, USA*, vol. 1, no. 19, 2011.

Kim, Tae-Sung, Byoung-Gun Park, Dong-Myung Lee, Ji-Su Ryu, and Dong-Seok Hyun. "A new approach to sensorless control method for brushless DC motors." *International Journal of Control, Automation, and Systems* 6, no. 4 (2008): 477-487.

Kottas, Theodoros L., Yiannis S. Boutalis, and Athanassios D. Karlis. "New maximum power point tracker for PV arrays using fuzzy controller in close cooperation with fuzzy cognitive networks." IEEE Transactions on Energy conversion 21, no. 3 (2006): 793-803.

Kumar, Rajan, and Bhim Singh. "BLDC motor-driven solar PV array-fed water pumping system employing zeta converter." *IEEE Transactions on Industry Applications* 52, no. 3 (2016): 2315-2322.

Kumar, Rajan, and Bhim Singh. "Solar PV powered BLDC motor drive for water pumping using Cuk converter." *IET Electric Power Applications* 11, no. 2 (2017): 222-232.

Kumar, Rajan, and Bhim Singh. "Solar PV-battery based hybrid water pumping system using BLDC motor drive." In *2016 IEEE 1st International Conference on Power Electronics, Intelligent Control and Energy Systems (ICPEICES)*, pp. 1-6. IEEE, 2016.

Li, X., Li, Y., Seem, J. E., & Lei, P. (2011, January). Maximum power point tracking for photovoltaic systems using adaptive extremum seeking control. In *Dynamic Systems and Control Conference* (Vol. 54754, pp. 803-810).

Liu, F., Kang, Y., Zhang, Y., & Duan, S. (2008, June). Comparison of P&O and hill climbing MPPT methods for grid-connected PV converter. In *2008 3rd IEEE Conference on Industrial Electronics and Applications* (pp. 804-807). IEEE.

Murshid, Shadab, and Bhim Singh. "Reduced sensor-based PMSM driven autonomous solar water pumping system." IEEE Transactions on Sustainable Energy 11, no. 3 (2019): 1323-1331.

Murshid, Shadab, and Bhim Singh. "Power quality improvement in grid integrated solar water pumping system using Vienna converter." *International Transactions on Electrical Energy Systems* 29, no. 12 (2019): e12129.

Nasser, K. W., Yaqoob, S. J., & Hassoun, Z. A. “Improved dynamic performance of photovoltaic panel using fuzzy logic-MPPT algorithm” *Indonesian Journal of Electrical Engineering and Computer Science*, vol.*21*, no.2, pp.617-624. 2021.

Nayak, B. K., Mohapatra, A., & Mohanty, K. B. (2013, December). Parameters estimation of photovoltaic module using nonlinear least square algorithm: A comparative study. In *2013 Annual IEEE India Conference (INDICON)* (pp. 1-6). IEEE.

P. Jena, R. Pudur, P. K. Ray, and A. Mohanty, “ANN Based MPPT Applied to Solar Powered Water Pumping System Using BLDC Motor,” in *1st IEEE International Conference on Sustainable Energy Technologies and Systems, ICSETS 2019*, Feb. 2019, pp. 200–205. doi: 10.1109/ICSETS.2019.8744804.

Pandiarajan, Natarajan, Ramabadran Ramaprabha, and Ranganath Muthu. "Application of circuit model for photovoltaic energy conversion system." *International Journal of Photoenergy* 2012 (2012).

Pal, N. Modeling and Simulation of Photovoltaic Arrays using Simple Mathematical Block by Matlab Simulink. *Int. J. Sci. Eng. Res.* **2014**, *5*, 658–663.

RASHEED, Mohammed, Suha SHIHAB, Taha RASHID, and Olfa Maalej. "Determining the Voltage and Power of a Single Diode PV Cell in Matlab by Iteration." *Journal of Al-Qadisiyah for Computer Science and Mathematics* 13, no. 1 (2021): Page-70.

Robles Algarín, Carlos, John Taborda Giraldo, and Omar Rodriguez Alvarez. "Fuzzy logic based MPPT controller for a PV system." *Energies* 10, no. 12 (2017): 2036.

R. Kumar and B. Singh, “BLDC Motor-Driven Solar PV Array-Fed Water Pumping System Employing Zeta Converter,” *IEEE Trans Ind Appl*, vol. 52, no. 3, pp. 2315–2322, May 2016, doi: 10.1109/TIA.2016.2522943.

Robles Algarín, Carlos, John Taborda Giraldo, and Omar Rodriguez Alvarez. "Fuzzy logic based MPPT controller for a PV system." *Energies* 10, no. 12 (2017): 2036.

R. Kumar and B. Singh, “BLDC Motor-Driven Solar PV Array-Fed Water Pumping System Employing Zeta Converter,” *IEEE Trans Ind Appl*, vol. 52, no. 3, pp. 2315–2322, May 2016, doi: 10.1109/TIA.2016.2522943.

Saleh, A. L., Obed, A. A., Hassoun, Z. A., & Yaqoob, S. J. “Modeling and Simulation of A Low Cost Perturb& Observe and Incremental Conductance MPPT Techniques In Proteus Software Based on Flyback Converter” In *IOP Conference Series: Materials Science and Engineering*, vol. 881, no. 1, p. 012152). IOP Publishing, Jul. 2020.

Shang, L., Guo, H., & Zhu, W. “An improved MPPT control strategy based on incremental conductance algorithm”. *Protection and Control of Modern Power Systems*, vol. *5*, no. 1, 1-8. 2020.

Sher, H. A., Murtaza, A. F., Noman, A., Addoweesh, K. E., Al-Haddad, K., & Chiaberge, M “A new sensorless hybrid MPPT algorithm based on fractional short-circuit current measurement and P&O MPPT” *IEEE Transactions on sustainable energy*, vol.*6*, no.4, 1426-1434. 2015.

Shetty, Prakhyath, AK Nitin Subramonium, and M. Sathyendra Kumar. "Mathematical modeling of permanent magnet brushless dc motor for electric scooter." In *2015 Fifth International Conference on Communication Systems and Network Technologies*, pp. 1222-1226. IEEE, 2015.

Shongwe, Samkeliso, and Moin Hanif. "Comparative analysis of different single-diode PV modeling methods." *IEEE Journal of photovoltaics* 5, no. 3 (2015): 938-946.

Thounthong P, Pierfederici S, Martin JP, Hinaje M, Davat B. Modeling and control of fuel cell/supercapacitor hybrid source based on differential flatness control. IEEE Transactions on Vehicular Technology. 2010 Mar 29;59(6):2700-10.

Tian, H.; Mancilla□David, F.; Ellis, K.; Muljadi, E.; Jenkins, P. A cell□to□module□to□array detailed model for photovoltaic panels. *Sol. Energy* **2012**, *86*, 2695–2706.

Yaqoob, Salam J., Saad Motahhir, and Ephraim Bonah Agyekum. "A new model for a photovoltaic panel using Proteus software tool under arbitrary environmental conditions." *Journal of Cleaner Production* 333 (2022): 130074.

Yaqoob, Salam Jabr, and Adel A. Obed. "Modeling, simulation and implementation of PV system by proteus based on two-diode model." *Journal of techniques* 1, no. 1 (2019): 39-51.

Yaqoob, Salam J., Ameer L. Saleh, Saad Motahhir, Ephraim B. Agyekum, Anand Nayyar, and Basit Qureshi. "Comparative study with practical validation of photovoltaic monocrystalline module for single and double diode models." *Scientific Reports* 11, no. 1 (2021): 1-14.

Yaqoob, S. J., Hussein, A. R., & Saleh, A. L. “Low Cost and Simple P&O-MPP Tracker Using Flyback Converter” *Solid State Technology*, vol.*63*, no. 6, 9676-9689. 2020.

Yap, K. Y., Sarimuthu, C. R., & Lim, J. M. Y. (2020). Artificial intelligence based MPPT techniques for solar power system: A review. *Journal of Modern Power Systems and Clean Energy*, *8*(6), 1043-1059.

Yaqoob SJ, Ferahtia S, Obed AA, Rezk H, Alwan NT, Zawbaa HM, Kamel S. Efficient Flatness Based Energy Management Strategy for Hybrid Supercapacitor/Lithium-ion Battery Power System. IEEE Access. 2022 Dec 16;10:132153-63.